
ESTIMATING KNOTS AND THEIR ASSOCIATION IN PARALLEL BILINEAR SPLINE GROWTH CURVE MODELS IN THE FRAMEWORK OF INDIVIDUAL MEASUREMENT OCCASIONS

Jin Liu *

Department of Biostatistics
Virginia Commonwealth University

Robert A. Perera

Department of Biostatistics
Virginia Commonwealth University

May 30, 2022

ABSTRACT

Latent growth curve models with spline functions are flexible and accessible statistical tools for investigating nonlinear change patterns that exhibit distinct phases of development in manifested variables. Among such models, the bilinear spline growth model (BLSGM) is the most straightforward and intuitive but useful. An existing study has demonstrated that the BLSGM allows the knot (or inflection point), at which two linear segments join together, to be an additional growth factor other than the intercept and slopes so that researchers can estimate the knot and its variability in the framework of individual measurement occasions. However, developmental processes are rarely isolated and the joint development where the change patterns of two constructs and their changes are related over time. As an extension of the existing BLSGM with an unknown knot, this study considers a parallel BLSGM (PBLSMG) for investigating two nonlinear growth processes and estimating the knot with its variability of each process as well as the knot-knot association in the framework of individual measurement occasions. We present the proposed model by simulation studies and a real-world data analysis. Our simulation studies demonstrate that the proposed PBLSGM generally estimate the parameters of interest unbiasedly, precisely and exhibit appropriate confidence interval coverage. An empirical example using longitudinal reading scores, mathematics scores and science scores shows that the model can estimate the knot with its variance for each growth curve and the covariance between two knots. We also provide the corresponding code for the proposed model.

Keywords Parallel Linear Spline Growth Models · Unknown Knots · Individually-varying Time Points · Simulation Studies

1 Introduction

Longitudinal analysis plays an essential role in various disciplines to investigate how the metrics of interest change over time. When analyzing such repeated measures, it is of interest to investigate the between-individual difference in within-individual change. The change patterns are likely to exhibit a nonconstant relationship to the time to some extent if the study duration under examination is long enough. One possible model to assess the individually nonlinear change pattern is the linear spline growth model (LSGM) (Grimm et al., 2016), which is also referred to as a piecewise linear latent growth model (Kohli, 2011; Kohli et al., 2013; Kohli and Harring, 2013; Sterba, 2014). With attached at least two linear pieces (see Figure A.1), the linear spline (or piecewise linear) growth curve is capable of approximating more complex underlying change patterns. It has been widely employed in multiple areas, for example, intellectual development (Marcoulides, 2018), the learning process of a specific task (Cudeck and Klebe, 2002), the onset of alcohol abuse (Li et al., 2001), and the post-surgical recovery process (Dumenci et al., 2019; Riddle et al., 2015).

When analyzing a growth curve model with a linear spline functional form, other than growth factors such as intercepts and slopes, the locations of the inflection points or ‘knots’ at which the change in the process has occurred must be

*CONTACT Jin Liu Email: Veronica.Liu0206@gmail.com

determined. Driven by domain theories, empirical researchers may pre-specify knot locations (Dumenci et al., 2019; Flora, 2008; Riddle et al., 2015; Sterba, 2014). Marcoulides (2018) also proposed a specification search by fitting a pool of candidate models and selecting the 'best' one using the BIC criterion. Kohli (2011); Kohli et al. (2013); Kohli and Harring (2013); Kohli et al. (2015a,b); Kwok et al. (2010); Liu (2019); Liu et al. (2019) have demonstrated that how to estimate knots in a much more flexible framework.

The simplest linear spline function is a bilinear spline growth model (BLSGM, or linear-linear piecewise model). This functional form helps identify a process that is theoretically to be two stages with different rates of change (Dumenci et al., 2019; Riddle et al., 2015; Liu, 2019); more importantly, it is also capable of approximating other nonlinear trajectories (Kohli et al., 2015a; Liu et al., 2019). Harring et al. (2006) developed a BLSGM to estimate a fixed knot with the assumption that the knot is at an identical point in time for all individuals. They unified the functional form of two linear pieces through reparameterization by re-expressing growth factors as linear combinations of their original form. The model has been proven useful for examining the development in each stage and estimating a fixed knot for procedural learning task research (Kohli and Harring, 2013). By relaxing the assumption of the same knot location across all individuals, Preacher and Hancock (2015) extended the BLSGM to estimate a knot and its variance simultaneously, where the knot is treated as an additional growth factor in addition to the intercept and two slopes. For interpretation purposes, Kohli (2011), Kohli et al. (2013), Grimm et al. (2016) and Liu (2019), Liu et al. (2019) provided the inverse-transformation matrices, which allow the reparameterized mean vector and variance-covariance matrix to be transformed back to the original parameterization, for the BLSGM with fixed and random knots, respectively.

However, developmental processes usually correlate with each other; accordingly, empirical researchers often desire to understand a joint development of at least two metrics of interest. One possible statistical method to analyze repeated measures of multiple constructs simultaneously is a parallel process and correlated growth model (McArdle, 1988), also referred to as a multivariate growth model (MGM) (Grimm et al., 2016). For example, Robitaille et al. (2012) detected a significant intercept-intercept and slope-slope association in processing speed and visuospatial ability by employing the MGM with linear growth curves. However, to our knowledge, no existing studies provide parallel nonlinear change patterns to assess at least two associated developmental processes. In this work, we propose parallel BLSGM (PBLSGM) by extending the BLSGM (Liu et al., 2019), which estimates a knot with its variance, to the multivariate growth model framework. With the PBLSGM, it is of interest to assess the knot-knot association other than the intercept-intercept and slope-slope association between at least two repeated outcomes. We also extend the transformation and inverse-transformation matrices of growth factors in the original and reparameterized settings developed in the Liu et al. (2019) to the PBLSGM, so the estimates can be directly interpreted.

Similar to Liu et al. (2019), we propose the PBLSGM in the framework of individual measurement occasions due to possible heterogeneity in the measurement occasions in a longitudinal study (Cook and Ware, 1983; Finkel et al., 2003; Mehta and West, 2000). This can occur when participants vary in age at each measurement occasion in developmental and aging studies where the response is most sensitive to changes in age rather than the measurement time. Another possible scenario of heterogeneity in the measurement occasion may result from when longitudinal responses are self-initiated. For example, in an adolescent smoking study, the longitudinal records were collected from questionnaires that were asked to complete on pocket computers immediately after smoking (Hedeker and Gibbons, 2006). We fit the proposed PBLSGM with individual measurement occasions using the definition variable approach, where the "definition variables" are defined as manifested variables that adjust model parameters to individual-specific values (Mehta and West, 2000; Mehta and Neale, 2005). In our case, these individual-specific values are individual measurement occasions. To our knowledge, this is the first study that demonstrates how to incorporate the definition variables in parallel growth curve models.

The proposed model fills an existing gap by describing how to fit a PBLSGM in the framework of individually-varying time points (ITPs) to estimate the knot with its variance for the growth curve of each repeated measures and the knot-knot association. In this current work, we have three major goals. First, we aim to capture characteristics of parallel individual trajectories with linear-linear piecewise functional form and analyze the associations between multiple developmental processes. More importantly, for the proposed model, we desire to make the statistical inference and interpret the estimates in the original parameter setting. Second, with the definition variable approach, we fit the model in the framework of individual measurement occasions due to its omnipresence in longitudinal studies. Third, we provide a set of recommendations for real-world practice by demonstrating how to apply the proposed model to a real data set.

The remainder of this article is organized as follows. In the method section, we first present the model specification of the PBLSGM to estimate a knot with its variance for the growth curve of each longitudinal response and the knot-knot association. Next, we extend the (inverse-)transformation matrix proposed by Liu (2019) to the PBLSGM framework and demonstrate how to parameterize growth factors in this model to make them estimable and transform them back after estimation for interpretation purposes. We also propose one possible reduced PBLSGM to estimate

knots without considering variability as a parsimonious backup. We next describe the model estimation and the Monte Carlo simulation design for model evaluation. In the section of the simulation result, we present the evaluation of the model performance in terms of non-convergent rate, the proportion of improper solutions, the estimating effects, which include the bias, the root-mean-squared-error (RSME) and the empirical coverage for a nominal 95% confidence interval of each parameter of interest. Then by applying the proposed PBLSGM to a data set of longitudinal reading scores, mathematics scores and science scores from the Early Childhood Longitudinal Study, Kindergarten Class of 2010 – 11 (ECLS-K: 2011), we provide a collection of feasible recommendations for empirical practice. Finally, discussions are framed regarding the model’s limitations as well as future directions.

2 Method

2.1 Model Specification

Suppose we have bivariate growth curves, in the framework of individual measurement occasions, the PBLSGM with unknown knots is given by

$$\begin{pmatrix} \mathbf{y}_i \\ \mathbf{z}_i \end{pmatrix} = \begin{pmatrix} \mathbf{\Lambda}_i(\gamma_i^{[y]}) & \mathbf{0} \\ \mathbf{0} & \mathbf{\Lambda}_i(\gamma_i^{[z]}) \end{pmatrix} \times \begin{pmatrix} \boldsymbol{\eta}_i^{[y]} \\ \boldsymbol{\eta}_i^{[z]} \end{pmatrix} + \begin{pmatrix} \boldsymbol{\epsilon}_i^{[y]} \\ \boldsymbol{\epsilon}_i^{[z]} \end{pmatrix}, \quad (1)$$

where \mathbf{y}_i and \mathbf{z}_i are $J \times 1$ vectors of the repeated outcomes \mathbf{Y} and \mathbf{Z} for the i^{th} person (where J is the number of measurements), respectively. $\mathbf{\Lambda}_i(\gamma_i^{[u]})$ ($u = y, z$), which is a function of an outcome-specific unknown knot $\gamma_i^{[u]}$, is a $J \times 3$ matrix of factor loadings determined by definition variables. $\boldsymbol{\eta}_i^{[u]}$ is a 3×1 vector of growth factors ($\boldsymbol{\eta}_i^{[u]} = (\eta_{0i}^{[u]}, \eta_{1i}^{[u]}, \eta_{2i}^{[u]})^T$, for an intercept and two slopes of the repeated outcome \mathbf{U}) of the i^{th} individual, which are further written as deviations from their outcome-specific means

$$\begin{pmatrix} \boldsymbol{\eta}_i^{[y]} \\ \boldsymbol{\eta}_i^{[z]} \end{pmatrix} = \begin{pmatrix} \boldsymbol{\mu}_{\boldsymbol{\eta}}^{[y]} \\ \boldsymbol{\mu}_{\boldsymbol{\eta}}^{[z]} \end{pmatrix} + \begin{pmatrix} \boldsymbol{\zeta}_i^{[y]} \\ \boldsymbol{\zeta}_i^{[z]} \end{pmatrix}, \quad (2)$$

where $\boldsymbol{\mu}_{\boldsymbol{\eta}}^{[u]}$ is a 3×1 vector of means of growth factors and $\boldsymbol{\zeta}_i^{[u]}$ is a 3×1 vector of deviations of the i^{th} subject from factor means of the repeated outcome \mathbf{U} . It is noted that $(\boldsymbol{\zeta}_i^{[y]} \ \boldsymbol{\zeta}_i^{[z]})^T$ follows a multivariate normal distribution

$$\begin{pmatrix} \boldsymbol{\zeta}_i^{[y]} \\ \boldsymbol{\zeta}_i^{[z]} \end{pmatrix} \sim MVN\left(\mathbf{0}, \begin{pmatrix} \boldsymbol{\Psi}_{0\boldsymbol{\eta}}^{[y]} & \boldsymbol{\Psi}_{0\boldsymbol{\eta}}^{[yz]} \\ \boldsymbol{\Psi}_{0\boldsymbol{\eta}}^{[yz]} & \boldsymbol{\Psi}_{0\boldsymbol{\eta}}^{[z]} \end{pmatrix}\right),$$

where $\boldsymbol{\Psi}_{0\boldsymbol{\eta}}^{[u]}$ is a 3×3 outcome-specific variance-covariance matrix of growth factors and $\boldsymbol{\Psi}_{0\boldsymbol{\eta}}^{[yz]}$ indicates the covariances between growth factors of repeated outcomes \mathbf{Y} and \mathbf{Z} .

In Equation (1), $\boldsymbol{\epsilon}_i^{[u]}$ is $J \times 1$ vector of outcome-specific residuals of the i^{th} person. To simplify the model, we assume that individual outcome-specific residuals follow identical and independent normal distributions over time and the covariance of residuals are homogeneous over time, that is,

$$\begin{pmatrix} \boldsymbol{\epsilon}_i^{[y]} \\ \boldsymbol{\epsilon}_i^{[z]} \end{pmatrix} \sim MVN\left(\mathbf{0}, \begin{pmatrix} \theta_{\epsilon}^{[y]} \mathbf{I} & \theta_{\epsilon}^{[yz]} \mathbf{I} \\ \theta_{\epsilon}^{[yz]} \mathbf{I} & \theta_{\epsilon}^{[z]} \mathbf{I} \end{pmatrix}\right).$$

In the model shown in Equation (1), the outcome-specific inflection point $\gamma_i^{[u]}$, like the outcome-specific intercept and slopes, varies across individuals and then viewed as an additional growth factor. This model, which specifies a nonlinear relationship between repeated outcomes and the growth factors, cannot be estimated in the structural equation modeling (SEM) framework directly (Grimm et al., 2016). Followed by Liu (2019); Liu et al. (2019), each repeated outcome in the proposed model can be reparameterized (Tishler and Zang, 1981; Seber and Wild, 2003; Liu, 2019; Liu et al., 2019) and then expressed as a linear combination of all four outcome-specific growth factors through the Taylor series expansion (Browne and du Toit, 1991; Grimm et al., 2016; Liu, 2019; Liu et al., 2019) (see Appendix A.1 and A.2 for details of reparameterization and Taylor series expansion).

We then express the outcome-specific reparameterized growth factors and the corresponding factor loadings for the i^{th} individual as

$$\boldsymbol{\eta}_i'^{[u]} = \begin{pmatrix} \eta_{0i}'^{[u]} & \eta_{1i}'^{[u]} & \eta_{2i}'^{[u]} & \delta_i^{[u]} \end{pmatrix}^T = \begin{pmatrix} \eta_{0i}^{[u]} + \gamma_i^{[u]} \eta_{1i}^{[u]} & \frac{\eta_{1i}^{[u]} + \eta_{2i}^{[u]}}{2} & \frac{\eta_{2i}^{[u]} - \eta_{1i}^{[u]}}{2} & \gamma_i^{[u]} - \mu_{\gamma}^{[u]} \end{pmatrix}^T \quad (3)$$

and

$$\boldsymbol{\Lambda}'_i(\gamma_i^{[u]}) = \begin{pmatrix} 1 & t_{ij} - \mu_\gamma^{[u]} & |t_{ij} - \mu_\gamma^{[u]}| & -\mu_{\eta_2}^{[u]} - \frac{\mu_{\eta_2}'^{[u]}(t_{ij} - \mu_\gamma^{[u]})}{|t_{ij} - \mu_\gamma^{[u]}|} \end{pmatrix} \quad (j = 1, \dots, J), \quad (4)$$

respectively, where $\mu_\gamma^{[u]}$ is the outcome-specific knot mean and $\delta_i^{[u]}$ is the deviation from the knot mean of the i^{th} individual. With $\boldsymbol{\eta}_i^{[u]}$ and $\boldsymbol{\Lambda}'_i(\gamma_i^{[u]})$ as shown in Equations (3) and (4), we then respecify the PBLSGM in Equations (1) and (2) as

$$\begin{pmatrix} \mathbf{y}_i \\ \mathbf{z}_i \end{pmatrix} = \begin{pmatrix} \boldsymbol{\Lambda}'_i(\gamma_i^{[y]}) & \mathbf{0} \\ \mathbf{0} & \boldsymbol{\Lambda}'_i(\gamma_i^{[z]}) \end{pmatrix} \times \begin{pmatrix} \boldsymbol{\eta}_i^{[y]} \\ \boldsymbol{\eta}_i^{[z]} \end{pmatrix} + \begin{pmatrix} \boldsymbol{\epsilon}_i^{[y]} \\ \boldsymbol{\epsilon}_i^{[z]} \end{pmatrix} \quad (5)$$

and

$$\begin{pmatrix} \boldsymbol{\eta}_i^{[y]} \\ \boldsymbol{\eta}_i^{[z]} \end{pmatrix} = \begin{pmatrix} \boldsymbol{\mu}_\eta^{[y]} \\ \boldsymbol{\mu}_\eta^{[z]} \end{pmatrix} + \begin{pmatrix} \boldsymbol{\zeta}_i^{[y]} \\ \boldsymbol{\zeta}_i^{[z]} \end{pmatrix}, \quad (6)$$

respectively, where $\boldsymbol{\mu}_\eta^{[u]}$ is a 4×1 vector of outcome-specific reparameterized growth factor means and $\boldsymbol{\zeta}_i^{[u]}$ is a 4×1 vector of normally distributed deviations of the i^{th} individual from the reparameterized growth factor means.

2.2 Transformation Matrix and Inverse-transformation Matrix

A set of reasonable initial values usually helps expedite the computational process and increase the likelihood of convergence when fitting a complex model in the SEM framework. Descriptive statistics and visualization are useful tools for empirical researchers to decide proper initial values for the parameters. However, this decision is not straightforward for the reparameterized parameters. To help select initial values, Liu et al. (2019) proposed transformation matrices to re-express the mean vector and variance-covariance matrix of growth factors in the original setting as those in the reparameterized setting for a BLSGM to estimate an unknown knot with its variability. They also developed inverse-transformation matrices to transform the mean vector and variance-covariance matrix of reparameterized growth factors to the original setting so the estimates are interpretable. By extending that work, we demonstrate how to implement these (inverse-)transformation matrices in the PBLSGM.

As shown in Equation (3), for the i^{th} individual, the relationship between the outcome-specific growth factors in the original setting ($\boldsymbol{\eta}_i^{[u]}$) and those in the reparameterized framework ($\boldsymbol{\eta}_i^{[u]}$) are $\mathbf{G}_i^{[u]}$ and $\mathbf{G}_i^{-1[u]}$ that are given by

$$\begin{aligned} \boldsymbol{\eta}_i^{[u]} &= \begin{pmatrix} \eta_{0i}^{[u]} & \eta_{1i}^{[u]} & \eta_{2i}^{[u]} & \delta_i^{[u]} \end{pmatrix}^T = \begin{pmatrix} \eta_{0i}^{[u]} + \gamma_i^{[u]} \eta_{1i}^{[u]} & \frac{\eta_{1i}^{[u]} + \eta_{2i}^{[u]}}{2} & \frac{\eta_{2i}^{[u]} - \eta_{1i}^{[u]}}{2} & \gamma_i^{[u]} - \mu_\gamma^{[u]} \end{pmatrix}^T \\ &= \begin{pmatrix} 1 & \gamma_i^{[u]} & 0 & 0 \\ 0 & 0.5 & 0.5 & 0 \\ 0 & -0.5 & 0.5 & 0 \\ 0 & 0 & 0 & 1 \end{pmatrix} \begin{pmatrix} \eta_{0i}^{[u]} \\ \eta_{1i}^{[u]} \\ \eta_{2i}^{[u]} \\ \gamma_i^{[u]} - \mu_\gamma^{[u]} \end{pmatrix} = \mathbf{G}_i^{[u]} \times \begin{pmatrix} \eta_{0i}^{[u]} \\ \eta_{1i}^{[u]} \\ \eta_{2i}^{[u]} \\ \gamma_i^{[u]} - \mu_\gamma^{[u]} \end{pmatrix} \end{aligned}$$

and

$$\begin{aligned} \boldsymbol{\eta}_i^{[u]} &= \begin{pmatrix} \eta_{0i}^{[u]} & \eta_{1i}^{[u]} & \eta_{2i}^{[u]} & \gamma_i^{[u]} \end{pmatrix}^T = \begin{pmatrix} \eta_{0i}^{[u]} - \gamma_i^{[u]} \eta_{1i}^{[u]} + \gamma_i^{[u]} \eta_{2i}^{[u]} & \eta_{1i}^{[u]} - \eta_{2i}^{[u]} & \eta_{1i}^{[u]} + \eta_{2i}^{[u]} & \delta_i^{[u]} + \mu_\gamma^{[u]} \end{pmatrix}^T \\ &= \begin{pmatrix} 1 & -\gamma_i^{[u]} & \gamma_i^{[u]} & 0 \\ 0 & 1 & -1 & 0 \\ 0 & 1 & 1 & 0 \\ 0 & 0 & 0 & 1 \end{pmatrix} \begin{pmatrix} \eta_{0i}^{[u]} \\ \eta_{1i}^{[u]} \\ \eta_{2i}^{[u]} \\ \delta_i^{[u]} + \mu_\gamma^{[u]} \end{pmatrix} = \mathbf{G}_i^{-1[u]} \times \begin{pmatrix} \eta_{0i}^{[u]} \\ \eta_{1i}^{[u]} \\ \eta_{2i}^{[u]} \\ \delta_i^{[u]} + \mu_\gamma^{[u]} \end{pmatrix}. \end{aligned}$$

The outcome-specific (inverse-)transformation matrix, like the matrix of BLSGM (Liu et al., 2019), is individual-level due to the knot variability. Liu et al. (2019) then introduced the population-level (inverse-)transformation matrix to simplify the calculation and showed that the most critical condition to apply the population-level transformation is when the variance of the knot approaches 0. By simulation studies, they demonstrated that the biases were still trivial though increased with an increasing knot variance. Therefore, in this current work, we still employ the population-level (inverse-) transformation matrix for each repeated outcome.

The outcome-specific transformation and inverse-transformation matrix between the mean vector of the outcome-specific original growth factors ($\boldsymbol{\mu}_{\boldsymbol{\eta}}^{[u]}$) and that of the reparameterized growth factors ($\boldsymbol{\mu}_{\boldsymbol{\eta}'}^{[u]}$) are

$$\boldsymbol{\mu}_{\boldsymbol{\eta}'}^{[u]} \approx \begin{pmatrix} 1 & \mu_{\gamma}^{[u]} & 0 & 0 \\ 0 & 0.5 & 0.5 & 0 \\ 0 & -0.5 & 0.5 & 0 \\ 0 & 0 & 0 & 1 \end{pmatrix} \times \begin{pmatrix} \mu_{\eta_0}^{[u]} \\ \mu_{\eta_1}^{[u]} \\ \mu_{\eta_2}^{[u]} \\ 0 \end{pmatrix} = \mathbf{G}^{[u]} \times \begin{pmatrix} \mu_{\eta_0}^{[u]} \\ \mu_{\eta_1}^{[u]} \\ \mu_{\eta_2}^{[u]} \\ 0 \end{pmatrix}$$

and

$$\boldsymbol{\mu}_{\boldsymbol{\eta}}^{[u]} \approx \begin{pmatrix} 1 & -\mu_{\gamma}^{[u]} & \mu_{\gamma}^{[u]} & 0 \\ 0 & 1 & -1 & 0 \\ 0 & 1 & 1 & 0 \\ 0 & 0 & 0 & 1 \end{pmatrix} \times \begin{pmatrix} \mu_{\eta_0'}^{[u]} \\ \mu_{\eta_1'}^{[u]} \\ \mu_{\eta_2'}^{[u]} \\ \mu_{\gamma}^{[u]} \end{pmatrix} = \mathbf{G}^{-1[u]} \times \begin{pmatrix} \mu_{\eta_0'}^{[u]} \\ \mu_{\eta_1'}^{[u]} \\ \mu_{\eta_2'}^{[u]} \\ \mu_{\gamma}^{[u]} \end{pmatrix},$$

respectively. We then express the transformation and inverse-transformation matrix between the variance-covariance matrix of the original growth factors and that of reparameterized growth factors as

$$\begin{aligned} \begin{pmatrix} \boldsymbol{\Psi}_{\boldsymbol{\eta}}'^{[y]} & \boldsymbol{\Psi}_{\boldsymbol{\eta}}'^{[yz]} \\ \boldsymbol{\Psi}_{\boldsymbol{\eta}}'^{[z]} \end{pmatrix} &\approx \begin{pmatrix} \nabla \mathbf{G}^{[y]} & \mathbf{0} \\ \nabla \mathbf{G}^{[z]} & \mathbf{0} \end{pmatrix} \times \begin{pmatrix} \boldsymbol{\Psi}_{\boldsymbol{\eta}}^{[y]} & \boldsymbol{\Psi}_{\boldsymbol{\eta}}^{[yz]} \\ \boldsymbol{\Psi}_{\boldsymbol{\eta}}^{[z]} \end{pmatrix} \times \begin{pmatrix} \nabla \mathbf{G}^{[y]} & \mathbf{0} \\ \nabla \mathbf{G}^{[z]} & \mathbf{0} \end{pmatrix}^T \\ &= \begin{pmatrix} \nabla \mathbf{G}^{[y]} \times \boldsymbol{\Psi}_{\boldsymbol{\eta}}^{[y]} \times \nabla \mathbf{G}^{[y]T} & \nabla \mathbf{G}^{[y]} \times \boldsymbol{\Psi}_{\boldsymbol{\eta}}^{[yz]} \times \nabla \mathbf{G}^{[z]T} \\ \nabla \mathbf{G}^{[z]} \times \boldsymbol{\Psi}_{\boldsymbol{\eta}}^{[yz]} \times \nabla \mathbf{G}^{[y]T} & \nabla \mathbf{G}^{[z]} \times \boldsymbol{\Psi}_{\boldsymbol{\eta}}^{[z]} \times \nabla \mathbf{G}^{[z]T} \end{pmatrix} \end{aligned}$$

and

$$\begin{aligned} \begin{pmatrix} \boldsymbol{\Psi}_{\boldsymbol{\eta}}^{[y]} & \boldsymbol{\Psi}_{\boldsymbol{\eta}}^{[yz]} \\ \boldsymbol{\Psi}_{\boldsymbol{\eta}}^{[z]} \end{pmatrix} &\approx \begin{pmatrix} \nabla \mathbf{G}^{-1[y]} & \mathbf{0} \\ \nabla \mathbf{G}^{-1[z]} & \mathbf{0} \end{pmatrix} \times \begin{pmatrix} \boldsymbol{\Psi}_{\boldsymbol{\eta}'}^{[y]} & \boldsymbol{\Psi}_{\boldsymbol{\eta}'}^{[yz]} \\ \boldsymbol{\Psi}_{\boldsymbol{\eta}'}^{[z]} \end{pmatrix} \times \begin{pmatrix} \nabla \mathbf{G}^{-1[y]} & \mathbf{0} \\ \nabla \mathbf{G}^{-1[z]} & \mathbf{0} \end{pmatrix}^T \\ &= \begin{pmatrix} \nabla \mathbf{G}^{-1[y]} \times \boldsymbol{\Psi}_{\boldsymbol{\eta}'}^{[y]} \times \nabla \mathbf{G}^{-1[y]T} & \nabla \mathbf{G}^{-1[y]} \times \boldsymbol{\Psi}_{\boldsymbol{\eta}'}^{[yz]} \times \nabla \mathbf{G}^{-1[z]T} \\ \nabla \mathbf{G}^{-1[z]} \times \boldsymbol{\Psi}_{\boldsymbol{\eta}'}^{[yz]} \times \nabla \mathbf{G}^{-1[y]T} & \nabla \mathbf{G}^{-1[z]} \times \boldsymbol{\Psi}_{\boldsymbol{\eta}'}^{[z]} \times \nabla \mathbf{G}^{-1[z]T} \end{pmatrix}, \end{aligned}$$

respectively, where $\boldsymbol{\Psi}_{\boldsymbol{\eta}}^{[u]}$ ($u = y, z$) and $\boldsymbol{\Psi}_{\boldsymbol{\eta}'}^{[u]}$ ($u = y, z$) are 4×4 outcome-specific variance-covariance matrix of original growth factors (an intercept, two slopes and a knot) and those of reparameterized growth factors, respectively. $\boldsymbol{\Psi}_{\boldsymbol{\eta}}^{[yz]}$ and $\boldsymbol{\Psi}_{\boldsymbol{\eta}'}^{[yz]}$ indicate the covariances between growth factors of repeated outcomes \mathbf{Y} and \mathbf{Z} in the original and reparameterized framework, respectively.

We only need to provide the matrices $\mathbf{G}^{[u]}$, $\mathbf{G}^{-1[u]}$, $\nabla \mathbf{G}^{[u]}$ and $\nabla \mathbf{G}^{-1[u]}$ for the transformation between the outcome-specific growth factors of the original setting and the reparameterized frame when fitting the PBLSGM using software such as the *R* package *OpenMx* that allows for matrix calculation. However, we need to give an expression of each cell of the mean vector and the variance-covariance matrices if (inversely) transforming parameters using SEM software that does not allow matrix algebra such as *Mplus*. We provide these expressions in Appendix A.3.

2.3 Model Estimation

For the i^{th} individual, the expected mean vector and the variance-covariance matrix of the bivariate repeated outcomes of the model given in Equation (5) and (6) can be expressed as

$$\boldsymbol{\mu}_i = \begin{pmatrix} \boldsymbol{\mu}_i^{[y]} \\ \boldsymbol{\mu}_i^{[z]} \end{pmatrix} = \begin{pmatrix} \boldsymbol{\Lambda}'_i(\gamma_i^{[y]}) & \mathbf{0} \\ \mathbf{0} & \boldsymbol{\Lambda}'_i(\gamma_i^{[z]}) \end{pmatrix} \times \begin{pmatrix} \boldsymbol{\mu}_{\boldsymbol{\eta}'}^{[y]} \\ \boldsymbol{\mu}_{\boldsymbol{\eta}'}^{[z]} \end{pmatrix} \quad (7)$$

and

$$\begin{aligned} \boldsymbol{\Sigma}_i &= \begin{pmatrix} \boldsymbol{\Sigma}_i^{[y]} & \boldsymbol{\Sigma}_i^{[yz]} \\ \boldsymbol{\Sigma}_i^{[z]} & \boldsymbol{\Sigma}_i^{[z]} \end{pmatrix} \\ &= \begin{pmatrix} \boldsymbol{\Lambda}'_i(\gamma_i^{[y]}) & \mathbf{0} \\ \mathbf{0} & \boldsymbol{\Lambda}'_i(\gamma_i^{[z]}) \end{pmatrix} \times \begin{pmatrix} \boldsymbol{\Psi}_{\boldsymbol{\eta}'}^{[y]} & \boldsymbol{\Psi}_{\boldsymbol{\eta}'}^{[yz]} \\ \boldsymbol{\Psi}_{\boldsymbol{\eta}'}^{[z]} & \boldsymbol{\Psi}_{\boldsymbol{\eta}'}^{[z]} \end{pmatrix} \times \begin{pmatrix} \boldsymbol{\Lambda}'_i(\gamma_i^{[y]}) & \mathbf{0} \\ \mathbf{0} & \boldsymbol{\Lambda}'_i(\gamma_i^{[z]}) \end{pmatrix}^T + \begin{pmatrix} \theta_{\epsilon}^{[y]} \mathbf{I} & \theta_{\epsilon}^{[yz]} \mathbf{I} \\ \theta_{\epsilon}^{[z]} \mathbf{I} & \theta_{\epsilon}^{[z]} \mathbf{I} \end{pmatrix}. \end{aligned} \quad (8)$$

The parameters in the model given in Equations (5) and (6) include the mean vector and the variance-covariance matrix of outcome-specific reparameterized growth factors, the reparameterized growth factor covariances, the outcome-specific residual variance and the residual covariance. Then we can calculate the parameters in the original setting with the inverse-transformation matrices proposed in Section 2.2. Θ_1 and Θ'_1 in Equations

$$\begin{aligned}\Theta_1 &= \{\boldsymbol{\mu}_{\boldsymbol{\eta}}^{[u]}, \boldsymbol{\Psi}_{\boldsymbol{\eta}}^{[u]}, \boldsymbol{\Psi}_{\boldsymbol{\eta}}^{[yz]}, \theta_{\epsilon}^{[u]}, \theta_{\epsilon}^{[yz]}\} \\ &= \{\mu_{\eta_0}^{[u]}, \mu_{\eta_1}^{[u]}, \mu_{\eta_2}^{[u]}, \mu_{\gamma}^{[u]}, \psi_{00}^{[u]}, \psi_{01}^{[u]}, \psi_{02}^{[u]}, \psi_{0\gamma}^{[u]}, \psi_{11}^{[u]}, \psi_{12}^{[u]}, \psi_{1\gamma}^{[u]}, \psi_{22}^{[u]}, \psi_{2\gamma}^{[u]}, \psi_{\gamma\gamma}^{[u]}, \\ &\quad \psi_{00}^{[yz]}, \psi_{01}^{[yz]}, \psi_{02}^{[yz]}, \psi_{0\gamma}^{[yz]}, \psi_{10}^{[yz]}, \psi_{11}^{[yz]}, \psi_{12}^{[yz]}, \psi_{1\gamma}^{[yz]}, \psi_{20}^{[yz]}, \psi_{21}^{[yz]}, \psi_{22}^{[yz]}, \psi_{2\gamma}^{[yz]}, \\ &\quad \psi_{\gamma 0}^{[yz]}, \psi_{\gamma 1}^{[yz]}, \psi_{\gamma 2}^{[yz]}, \psi_{\gamma\gamma}^{[yz]}, \theta_{\epsilon}^{[u]}, \theta_{\epsilon}^{[yz]}\} \\ &u = y, z\end{aligned}\quad (9)$$

and

$$\begin{aligned}\Theta'_1 &= \{\boldsymbol{\mu}'_{\boldsymbol{\eta}}^{[u]}, \boldsymbol{\Psi}'_{\boldsymbol{\eta}}^{[u]}, \boldsymbol{\Psi}'_{\boldsymbol{\eta}}^{[yz]}, \theta_{\epsilon}^{[u]}, \theta_{\epsilon}^{[yz]}\} \\ &= \{\mu'_{\eta_0}^{[u]}, \mu'_{\eta_1}^{[u]}, \mu'_{\eta_2}^{[u]}, \mu'_{\gamma}^{[u]}, \psi'_{00}^{[u]}, \psi'_{01}^{[u]}, \psi'_{02}^{[u]}, \psi'_{0\gamma}^{[u]}, \psi'_{11}^{[u]}, \psi'_{12}^{[u]}, \psi'_{1\gamma}^{[u]}, \psi'_{22}^{[u]}, \psi'_{2\gamma}^{[u]}, \psi'_{\gamma\gamma}^{[u]}, \\ &\quad \psi'_{00}^{[yz]}, \psi'_{01}^{[yz]}, \psi'_{02}^{[yz]}, \psi'_{0\gamma}^{[yz]}, \psi'_{10}^{[yz]}, \psi'_{11}^{[yz]}, \psi'_{12}^{[yz]}, \psi'_{1\gamma}^{[yz]}, \psi'_{20}^{[yz]}, \psi'_{21}^{[yz]}, \psi'_{22}^{[yz]}, \psi'_{2\gamma}^{[yz]}, \\ &\quad \psi'_{\gamma 0}^{[yz]}, \psi'_{\gamma 1}^{[yz]}, \psi'_{\gamma 2}^{[yz]}, \psi'_{\gamma\gamma}^{[yz]}, \theta_{\epsilon}^{[u]}, \theta_{\epsilon}^{[yz]}\} \\ &u = y, z\end{aligned}\quad (10)$$

list the parameters in the original and the reparameterized frame, respectively.

Θ'_1 is estimated using full information maximum likelihood (FIML) technique to account for the potential heterogeneity of individual contributions to the likelihood function. The log-likelihood function of each individual and that of the overall sample can be expressed as

$$\log lik_i(\Theta'_1 | \mathbf{y}_i, \mathbf{z}_i) = C - \frac{1}{2} \ln \begin{vmatrix} \boldsymbol{\Sigma}_i^{[y]} & \boldsymbol{\Sigma}_i^{[yz]} \\ \boldsymbol{\Sigma}_i^{[z]} & \boldsymbol{\Sigma}_i^{[z]} \end{vmatrix} - \frac{1}{2} \left(\begin{pmatrix} \mathbf{y}_i - \boldsymbol{\mu}_i^{[y]} \\ \mathbf{z}_i - \boldsymbol{\mu}_i^{[z]} \end{pmatrix}^T \begin{pmatrix} \boldsymbol{\Sigma}_i^{[y]} & \boldsymbol{\Sigma}_i^{[yz]} \\ \boldsymbol{\Sigma}_i^{[z]} & \boldsymbol{\Sigma}_i^{[z]} \end{pmatrix}^{-1} \begin{pmatrix} \mathbf{y}_i - \boldsymbol{\mu}_i^{[y]} \\ \mathbf{z}_i - \boldsymbol{\mu}_i^{[z]} \end{pmatrix} \right) \quad (11)$$

and

$$\log lik(\Theta'_1 | \mathbf{Y}, \mathbf{Z}) = \sum_{i=1}^n \log lik_i(\Theta'_1 | \mathbf{y}_i, \mathbf{z}_i), \quad (12)$$

respectively, where C is a constant, n is the number of individuals, and other parameters have been defined in Equations (7) and (8), respectively. We construct the proposed PBLSGM using the R package *OpenMx* with the optimizer CSOLNP (Neale et al., 2016; Pritikin et al., 2015; Hunter, 2018; Boker et al., 2018), with which we are capable of fitting the proposed model and carrying out the transformation matrix as well as inverse-transformation matrix as shown in Section 2.2 efficiently.

2.4 Reduced Model

A reduced model can be created with the assumption that the inflection point is roughly similar for each individual. We then fix the between-individual difference in each knot to 0, the model in Equation (1) has a reduced form for estimating unknown knots without variability, given by

$$\begin{pmatrix} \mathbf{y}_i \\ \mathbf{z}_i \end{pmatrix} = \begin{pmatrix} \boldsymbol{\Lambda}_i(\gamma^{[y]}) & \mathbf{0} \\ \mathbf{0} & \boldsymbol{\Lambda}_i(\gamma^{[z]}) \end{pmatrix} \times \begin{pmatrix} \boldsymbol{\eta}_i^{[y]} \\ \boldsymbol{\eta}_i^{[z]} \end{pmatrix} + \begin{pmatrix} \boldsymbol{\epsilon}_i^{[y]} \\ \boldsymbol{\epsilon}_i^{[z]} \end{pmatrix}, \quad (13)$$

where $\boldsymbol{\Lambda}_i(\gamma^{[u]})$, which is a function of the outcome-specific fixed knot $\gamma^{[u]}$, is a $J \times 3$ matrix of factor loadings.

This reduced PBLSGM also needs to reparameterized to have a unified linear combination of outcome-specific growth factors when being modeled in the SEM framework. Multiple approaches are available to realize the reparameterization process (Harring et al., 2006; Grimm et al., 2016). In this article, we express the outcome-specific repeated outcome as we did in Equation (A.1) and accordingly write the reparameterized growth factors and the corresponding factor loadings as

$$\boldsymbol{\eta}_i^{[u]} = \begin{pmatrix} \eta_{0i}^{[u]} & \eta_{1i}^{[u]} & \eta_{2i}^{[u]} \end{pmatrix}^T = \begin{pmatrix} \eta_{0i}^{[u]} + \gamma^{[u]} \eta_{1i}^{[u]} & \frac{\eta_{1i}^{[u]} + \eta_{2i}^{[u]}}{2} & \frac{\eta_{2i}^{[u]} - \eta_{1i}^{[u]}}{2} \end{pmatrix}^T \quad (14)$$

and

$$\boldsymbol{\Lambda}_i'(\gamma^{[u]}) = \begin{pmatrix} 1 & t_{ij} - \gamma^{[u]} & |t_{ij} - \gamma^{[u]}| \end{pmatrix} \quad (j = 1, \dots, J). \quad (15)$$

We also need to reduce transformation and inverse-transformation accordingly. Specifically, we only need the first three rows and the first three columns of such block matrix functions as $\mathbf{G}^{[u]}$, $\mathbf{G}^{-1[u]}$, $\nabla\mathbf{G}^{[u]}$ and $\nabla\mathbf{G}^{-1[u]}$, since only three growth factors for each repeated outcome need to be reparameterized.

With the reparameterized growth factors and the corresponding factor loadings as defined in Equations (14) and (15), for the i^{th} individual, the expected mean vector and the variance-covariance matrix of the repeated outcomes of the reduce PBLSGM are given by

$$\boldsymbol{\mu}_i = \begin{pmatrix} \boldsymbol{\mu}_i^{[y]} \\ \boldsymbol{\mu}_i^{[z]} \end{pmatrix} = \begin{pmatrix} \boldsymbol{\Lambda}'_i(\gamma^{[y]}) & \mathbf{0} \\ \mathbf{0} & \boldsymbol{\Lambda}'_i(\gamma^{[z]}) \end{pmatrix} \times \begin{pmatrix} \boldsymbol{\mu}_{\boldsymbol{\eta}'}^{[y]} \\ \boldsymbol{\mu}_{\boldsymbol{\eta}'}^{[z]} \end{pmatrix} \quad (16)$$

and

$$\begin{aligned} \boldsymbol{\Sigma}_i &= \begin{pmatrix} \boldsymbol{\Sigma}_i^{[y]} & \boldsymbol{\Sigma}_i^{[yz]} \\ \boldsymbol{\Sigma}_i^{[z]} & \boldsymbol{\Sigma}_i^{[z]} \end{pmatrix} \\ &= \begin{pmatrix} \boldsymbol{\Lambda}'_i(\gamma^{[y]}) & \mathbf{0} \\ \mathbf{0} & \boldsymbol{\Lambda}'_i(\gamma^{[z]}) \end{pmatrix} \times \begin{pmatrix} \boldsymbol{\Psi}'_{\boldsymbol{\eta}}^{[y]} & \boldsymbol{\Psi}'_{\boldsymbol{\eta}}^{[yz]} \\ \boldsymbol{\Psi}'_{\boldsymbol{\eta}}^{[z]} & \boldsymbol{\Psi}'_{\boldsymbol{\eta}}^{[z]} \end{pmatrix} \times \begin{pmatrix} \boldsymbol{\Lambda}'_i(\gamma^{[y]}) & \mathbf{0} \\ \mathbf{0} & \boldsymbol{\Lambda}'_i(\gamma^{[z]}) \end{pmatrix}^T + \begin{pmatrix} \theta_{\epsilon}^{[y]} \mathbf{I} & \theta_{\epsilon}^{[yz]} \mathbf{I} \\ \theta_{\epsilon}^{[z]} \mathbf{I} & \theta_{\epsilon}^{[z]} \mathbf{I} \end{pmatrix}, \end{aligned} \quad (17)$$

respectively. For this reduced model, $\boldsymbol{\Theta}_2$ and $\boldsymbol{\Theta}'_2$ are defined as

$$\begin{aligned} \boldsymbol{\Theta}_2 &= \{\boldsymbol{\mu}_{\boldsymbol{\eta}}^{[u]}, \boldsymbol{\Psi}_{\boldsymbol{\eta}}^{[u]}, \boldsymbol{\Psi}_{\boldsymbol{\eta}}^{[yz]}, \theta_{\epsilon}^{[u]}, \theta_{\epsilon}^{[yz]}\} \\ &= \{\mu_{\eta_0}^{[u]}, \mu_{\eta_1}^{[u]}, \mu_{\eta_2}^{[u]}, \gamma^{[u]}, \psi_{00}^{[u]}, \psi_{01}^{[u]}, \psi_{02}^{[u]}, \psi_{11}^{[u]}, \psi_{12}^{[u]}, \psi_{22}^{[u]}, \\ &\quad \psi_{00}^{[yz]}, \psi_{01}^{[yz]}, \psi_{02}^{[yz]}, \psi_{10}^{[yz]}, \psi_{11}^{[yz]}, \psi_{12}^{[yz]}, \psi_{20}^{[yz]}, \psi_{21}^{[yz]}, \psi_{22}^{[yz]}, \theta_{\epsilon}^{[u]}, \theta_{\epsilon}^{[yz]}\} \\ &\quad u = y, z \end{aligned} \quad (18)$$

and

$$\begin{aligned} \boldsymbol{\Theta}'_2 &= \{\boldsymbol{\mu}_{\boldsymbol{\eta}}'^{[u]}, \boldsymbol{\Psi}_{\boldsymbol{\eta}}'^{[u]}, \boldsymbol{\Psi}_{\boldsymbol{\eta}}'^{[u]}, \theta_{\epsilon}'^{[u]}, \theta_{\epsilon}'^{[yz]}\} \\ &= \{\mu_{\eta_0}'^{[u]}, \mu_{\eta_1}'^{[u]}, \mu_{\eta_2}'^{[u]}, \gamma^{[u]}, \psi_{00}'^{[u]}, \psi_{01}'^{[u]}, \psi_{02}'^{[u]}, \psi_{11}'^{[u]}, \psi_{12}'^{[u]}, \psi_{22}'^{[u]}, \\ &\quad \psi_{00}'^{[yz]}, \psi_{01}'^{[yz]}, \psi_{02}'^{[yz]}, \psi_{10}'^{[yz]}, \psi_{11}'^{[yz]}, \psi_{12}'^{[yz]}, \psi_{20}'^{[yz]}, \psi_{21}'^{[yz]}, \psi_{22}'^{[yz]}, \theta_{\epsilon}'^{[u]}, \theta_{\epsilon}'^{[yz]}\} \\ &\quad u = y, z \end{aligned} \quad (19)$$

and list the parameters in the original and reparameterized setting, respectively. We then repaced $\boldsymbol{\Theta}'_1$ in Equations (11) and (12) with $\boldsymbol{\Theta}'_2$ and updated $\boldsymbol{\mu}_i$ and $\boldsymbol{\Sigma}_i$ as such defined in Equations (16) and (17) and obtained the log-likelihood function of each individual and that of the overall sample. We also constructed the reduced PBLSGM using the R package *OpenMx* with the optimizer CSOLNP and employed the FIML technique to estimate the parameters. We provide the *OpenMx* syntax for the proposed PBLSGM and its reduced form as well as a demonstration in the online appendix (https://github.com/Veronica0206/Extension_projects). We also provide *Mplus* 8 syntax for both models in the online appendix for researchers who are interested in using *Mplus*.

3 Model Evaluation

We evaluated the proposed PBLSGM using a Monte Carlo simulation study with two goals. The first goal was to examine the estimating effects of the proposed PBLSGM, including the bias ($Bias_{\hat{\theta}}(\hat{\theta}, \theta) = E_{\hat{\theta}}(\hat{\theta} - \theta)$), RMSE ($RMSE_{\hat{\theta}}(\hat{\theta}, \theta) = \sqrt{E_{\hat{\theta}}(\hat{\theta} - \theta)^2}$) and the empirical coverage for a nominal 95% confidence interval of each parameter of interest. The second goal is to see how the reduced model performed as a parsimonious backup of the full PBLSGM.

3.1 Design of Simulation Study

As an extension of an existing BLSGM proposed by Liu et al. (2019), the primary focus of this study was to investigate how the performance of PBLSGM affected by the correlation between the growth patterns of two repeated outcomes. Accordingly, we did not investigate some conditions, such as the knot variance and the standardized difference between two slopes, that have demonstrated a clear pattern with the model performance of BLSGM in Liu et al. (2019). Instead, we set the knot standard deviation as 0.3 to be a moderate level of individual difference in each knot, and we adjusted the standardized difference between two slopes to satisfy other conditions that are of more interest in this study. In

addition, as shown in Table 1, we considered ten scaled and equally spaced waves since Liu et al. (2019) has presented that the BLSGM performed decently under the conditions with ten repeated measures and fewer follow-up time only affect model performance slightly. Around each wave, we allowed a time-window with a width $(-0.25, +0.25)$, which was a ‘medium’ deviation as Coulombe et al. (2015), for individual measurement occasions. We also fixed the variance-covariance matrix of within-construct growth factors since this matrix usually changes with the measurement scale and the time scale. Besides, the outcome-specific growth factors were set to be positively correlated to a moderate degree ($\rho = 0.3$). Additionally, guided by several existing studies (Bauer and Curran, 2003; Kohli, 2011; Kohli et al., 2015b; Liu et al., 2019), we kept the index of dispersion (σ^2/μ) of each growth factor at a tenth scale.

=====
Insert Table 1 about here
=====

In the simulation design, we considered the between-construct growth factor correlation as positive (0.3), negative (-0.3) and zero to evaluate how the association between two growth curves affects the model performance of PBLGGM. Additionally, we examine several common change patterns as shown in Table 1 (Scenario 1, 2 and 3). For each scenario, we changed the knot locations (set the knots of the trajectories of two repeated outcomes to be the same or different) and one growth factor and fixed the other two growth factors to investigate how the trajectory shape impacts the model. For the precision of measurements, we considered $\theta_\epsilon^{[u]} = 1$ or $\theta_\epsilon^{[u]} = 2$ as two levels of homogeneous outcome-specific residual variances and set the residual correlation as 0.3. We also considered two levels of sample size.

3.2 Data Generation and Simulation Step

For each condition listed in Table 1, we carried out the following general steps for the simulation study of the proposed PBLGGM:

1. Generated growth factors for two repeated outcomes simultaneously with the prespecified mean vector and variance-covariance matrix shown in Table 1 using the R package *MASS* (Venables and Ripley, 2002).
2. Generated the time structure with $J = 10$ scaled and equally-spaced waves t_j and obtained ITPs: $t_{ij} \sim U(t_j - \Delta, t_j + \Delta)$ by allowing a time-window with a width $(-\Delta, \Delta)$ around each wave.
3. Calculated factor loadings for each individual of each construct from ITPs and the outcome-specific knot location.
4. Calculated values of the repeated outcomes for each endpoint based on corresponding growth factors, factor loadings, and residual variances.
5. Implemented both PBLGGM with unknown knots on the generated data set, estimated the parameters, constructed corresponding 95% Wald CIs.
6. Replicated the above steps until after obtaining 1,000 convergent solutions.

4 Results

4.1 Model Convergence and Proper Solution

We first examined the convergence rate and component fit measures of each condition before evaluating how the proposed PBLGGM performed in terms of estimating effects. The convergence² rate of each condition was investigated. Based on our simulation studies, the proposed PBLGGM and its reduced version converged satisfactorily (the convergence rate of the full PBLGGM achieved at least 97% for all conditions while that of its reduced version was 100%). Upon further investigation, the non-convergent solutions usually occurred under the conditions with zero between-construct growth factor covariances.

=====
Insert Table 2 about here
=====

We also examined the pattern of improper solutions, includes negative estimations of growth factor variances and/or out-of-range (i.e., beyond $[-1, 1]$) growth factor correlations. Table 2 demonstrates the number of improper solutions

²In this work, convergence is defined as to achieve *OpenMx* status code 0, which suggests a successful optimization, until up to 10 attempts with different sets of initial values (Neale et al., 2016).

yielded by the proposed model under all conditions, which include negative knot variances and its out-of-range (i.e., out of $[-1, 1]$) correlations with any other growth factors from the same or the other construct. From the table, we noted that the conditions with real parallel trajectories of two repeated outcomes (i.e., the conditions with Scenario 1 of which both slopes of one construct were set as the same with the other construct) suffered improper solutions less frequently though different first slopes (Scenario 2) or second slopes (Scenario 3) only affected the proportion of improper solution slightly. Additionally, the small sample size or less precise measurements increased the proportion of improper solutions. We replaced the PBLGGM with its reduced model for the model evaluation if such improper solutions emerged.

4.2 Estimating Effects

Tables 3 and 4 present the median (range) of the bias and RMSE³, respectively, for each parameter of interest across all conditions for the proposed PBLGGM and its reduced version. For each parameter of interest, we first estimated its bias/RMSE across 1,000 replications under each condition and then summarized its biases/RMSEs over all the conditions as the bias/RMSE median (range). As shown in Tables 3 and 4, both models yielded unbiased point estimates with small RMSEs for the growth factor means though the biases and RMSEs of growth factor variances and those of intercept-intercept, slope-slope and knot-knot covariances were slightly larger. We also note that the ranges of biases/RMSEs of the parameters from the full PBLGGM were narrower than those from its reduced version, especially for the growth factor variances and the intercept-intercept, slope-slope and knot-knot covariances, indicating that the full model generally produced estimates that were closer to the population values. On further investigation, despite the increase in biases of the reduced model, the precision of its estimates remains comparable.

=====

Insert Table 3 about here

=====

=====

Insert Table 4 about here

=====

We also present the biases generated by the proposed PBLGGM for each parameter of interest in PBLGGM under all conditions in Appendix B (Figures B.1, B.2 and B.3). From these plots, we observed the following interesting patterns. First, the magnitude or sign of the between-construct correlation seemed not to affect the model performance. Second, the non-zero difference in knot locations of two constructs affected the model performance, but such influence was different on two repeated outcomes. Specifically, the biases of the first slope mean and variance of Y inflated while those of the second slope mean and variance of Y deflated. However, it oppositely impacted those estimates of Z . Third, the trajectory shape did not affect the biases meaningfully, but less precise measurements increased the biases.

Table 5 presents the median (range) of the coverage probability (CP) of each parameter of interest for the proposed PBLGGMs. Both models exhibited proper CPs for the intercept means and variances, intercept-intercept covariance and slope means in general. However, only the full PBLGGM demonstrated decent coverages for other parameters of interest, including knot means and variances, slope variances, slope-slope covariances and knot-knot covariance.

5 Application

This section demonstrates how to employ the proposed PBLGGM to analyze real-world data sets to approximate nonlinear parallel change patterns and estimate an outcome-specific knot with its variability as well as knot-knot association. This application has two goals. We first compare the fitness of parallel bilinear spline functional form to that of three common parametric change patterns: parallel linear, quadratic and Jenss-Bayley growth curve. Then we demonstrate the scenarios under which we should employ the full PBLGGM rather than its reduced version in practice. We extract 400 students randomly from the Early Childhood Longitudinal Study Kindergarten Cohort: 2010-2011 (ECLS-K: 2011) with complete records of repeated reading IRT scaled scores, math IRT scaled scores, science IRT scaled scores and age at each wave⁴.

³The model performance under the conditions with 0 population value of between-construct correlation is of interest. It is noted that, under these conditions, the relative bias (RMSE) of those correlations would go infinity. We then presented absolute biases (RMSEs) of all parameters for consistency in this section and provided the summary of relative biases (RMSEs) in Appendix B.

⁴The total sample size of ECLS-K: 2011 is $n = 18174$. The number of entries after removing records with missing values (i.e., rows with any of NaN/-9/-8/-7/-1) is $n = 2290$.

ECLS-K: 2011 is a nationwide longitudinal study of US children registered in about 900 kindergarten programs starting from 2010 – 2011 school year. In ECLS-K: 2011, children's reading ability and mathematics ability was assessed in nine waves: fall and spring of kindergarten (2010 – 2011), first (2011 – 2012) and second (2012 – 2013) grade, respectively, as well as spring of 3rd (2014), 4th (2015) and 5th (2016), respectively. Only about 30% students were evaluated in the fall of 2011 and 2012 (Lê et al., 2011). The science assessment started from the spring of kindergarten round, and it was evaluated in eight waves accordingly. In the analysis, we used children's age (in month) instead of their grade to obtain individual measurement occasions. In the subsample, 51% and 49% of children were boys and girls, respectively. Additionally, 45%, 5%, 38%, 8% and 4% of students were White, Black, Hispanic, Asian and others. In this section, we constructed PBLGMS to analyze the joint development of reading and mathematics ability and that of mathematics and science skills.

5.1 Joint Development in Reading Ability and Mathematics Ability

For the joint development of reading and mathematics ability, we first fit the full parallel bilinear spline growth curve model and its reduced version as well as parallel trajectories with three parametric functional forms: parallel linear, quadratic and Jenss-Bayley. Figure 1 presents the model implied curves on the smooth line of the observed reading and math IRT scores. From the figure, the nonlinear functions generally fit better than the linear function. As shown in Figure 1, although all nonlinear models underestimated the reading ability, the PBLGMS fit better than the models with parallel parametric nonlinear curves to the first two or three measures. Additionally, only the quadratic growth curve and the Jenss-Bayley tended to underrate the mathematics ability of children in the early stage.

=====

Insert Figure 1 about here

=====

Table 6 provides the obtained estimated likelihood, information criteria (including AIC and BIC), and residuals of each parallel growth curve model. From the table, the full PBLGMS has the largest estimated likelihood, smallest AIC and BIC, as well as the smallest residual variances, which led unequivocally to the selection of the full PBLGMS as the 'best' model from the statistical perspective.

=====

Insert Table 6 about here

=====

Table 7 presents the estimates of parameters of interest for the joint development of reading and mathematics ability. Post-knot development in reading skills and mathematics skills slowed down substantially. On average, for the reading ability, the development rates were 2.030 and 0.678 per month in the pre- and post-knot stage, respectively. These rates for the mathematics ability were 1.787 and 0.737. The knot of the reading skills and mathematics skills was estimated at 95- and 100-month (both around 8-year old) on average. We also noted a positive association between the development of reading skills and that of mathematics skills, and the intercept-intercept, pre-knot slope-slope and knot-knot association were significant.

=====

Insert Table 7 about here

=====

We then standardized these covariances, the intercept-intercept, pre-knot slope-slope, post-knot slope-slope and knot-knot correlations were 0.75, 0.64, 0.34 and 0.59, respectively. It suggests that, on average, a child who was higher in reading ability tended to be higher in mathematics ability and vice versa. Additionally, on average, a child who was increasing more rapidly in reading ability tended to increase more rapidly in mathematics ability over time and vice versa. Moreover, a child who achieved the inflection point of the trajectory of reading ability earlier tended to arrive at the knot of the development curve of mathematics ability earlier and vice versa.

5.2 Joint Development in Mathematics Ability and Science Ability

To demonstrate more complex parallel nonlinear change patterns in practice, we also built PBLGMS to assess the joint development of mathematics and science ability. It is noted that the mathematics ability was assessed in nine waves, while the science ability was only evaluated in the eight waves (starting from the second round). The proposed PBLGMS is capable of addressing this issue since the outcome-specific growth factors were indicated by their own set of repeated measurements in model specification. For this analysis, we defined nine factor loadings for the trajectories

of mathematics and science ability of each kid from individual measurement occasions of nine waves and only specify the last eight loadings, which correspond to the second round to the ninth round measurements, to the science ability. We first fit the full PBLGGM and its reduced version and list the estimated likelihood, information criteria, and residuals of both models in Table 8.

From the table, the full PBLGGM has a larger estimated likelihood, smaller AIC and smaller residuals, but its BIC is larger than the corresponding value of its reduced version, suggesting that the fit information fails to lead unequivocal selection. Upon further investigation, the estimated knot variance of science ability was not significant. We then fit a mixed PBLGGM, in which we consider the inflection point of the development of mathematics ability was individual different but that of the growth curve of science ability was roughly similar for each individual, and listed its information in Table 8. The mixed PBLGGM is the ‘best’ one among three the parallel bilinear spline growth models from the statistical perspective.

=====
Insert Table 8 about here
=====

Table 9 presents the estimates of parameters of interest for the joint development of mathematics and science ability. The estimated trajectory of mathematics ability was the same as the trajectory obtained in the parallel growth model of reading and mathematics ability. Additionally, we noticed that post-knot development in science skills also slowed down. On average, the development rates were 0.839 and 0.575 per month in the pre- and post-knot stage, respectively. The knot of science ability was estimated at 100-month (also around 8-year old) on average. The intercept-intercept, pre-knot slope-slope and post-knot slope-slope correlations were 0.65, 0.60 and 0.26, respectively. It suggests that the initial status of mathematics and science ability, as well as the development rates of two abilities, were positively associated.

=====
Insert Table 9 about here
=====

6 Discussion

In this article, we presented a PBLGGM for assessing a joint development where the change patterns of each endpoint are nonlinear. With this model, we can estimate a knot with its variance of trajectories of each repeated outcome and the knot-knot association. We also proposed its reduced version, a more parsimonious option when the full model fails to converge or to generate proper solutions, or estimated knot variances are not significant. More importantly, we extended (inverse-) transformation matrices in an existing study to the PBLGGM framework to help select proper initial values and, in turn, accelerate the computational process as well as make a statistical inference and interpret the estimates in the original framework. For both PBLGGMs, we performed in-depth analyses in terms of the non-convergent rate, improper solutions, and estimating effects, including the bias, RMSE and coverage probability of each parameter of interest through simulation studies. We also illustrated the proposed models using an empirical data set obtained from a longitudinal study of reading, mathematics and science ability. The results demonstrate valuable capabilities of estimating the knots, their variances and covariance in the framework of individual measurement occasions as well as interpreting the estimates from the models.

Across all conditions in the simulation design, both PBLGGM converged satisfactorily—the convergence rate of the full model achieved at least 97% while that of the reduced model was 100%. Additionally, as shown in the application section, the full PBLGGM was capable of achieving convergence status without computational burdens. We also noticed that the full model might suffer an issue of improper solutions, including negative knot variances and out-of-range knot correlations with other growth factors, within- or between-constructs. It is not surprising since the knot variances were set at a moderate level, 0.3 in the simulation design. In terms of estimating effects, the full PBLGGM was capable of estimating the parameters unbiasedly, precisely and exhibiting appropriate empirical coverage of nominal 95% confidence intervals. The biases of estimates produced by its reduced form increased slightly, especially for the growth factor variances and covariances, which in turn affects the RMSEs and coverage probabilities somewhat. Accordingly, in empirical practice, we recommend employing the reduced model when the full version fails to converge or generate proper solutions though sometimes at a little cost of a small increase in bias.

We next illustrated how to use the proposed models on a subset with $n = 400$ from ECLS-K: 2011 hoping to show the procedure and provide a set of recommendations for possible issues that empirical researchers may face in practice. First, proper research questions need to be raised before conducting any analysis. These questions include whether

or not to test associations between two endpoints and their nonlinear change patterns and for each repeated outcome, whether the research interest lies in to estimate a knot and its variance or fit nonlinear trajectories. It is worth considering either the full, reduced or mixed PBLSGM to estimate knots of a joint developmental process if it is the research interest. If the interest lies in to fit multivariate nonlinear development processes, it may be appropriate to fit the parallel change patterns with several functional forms and the selected ‘best’ one. Though the fit information led to unequivocal selection in our empirical examples, it is not always the case. Other criteria, such as the fit between the model-implied curve and the smooth line of the observed repeated outcome, also helps make a decision. In the first empirical case, for example, the PBLSGMs are better if it is important to capture children’s reading ability and mathematics ability in the early stage of the study.

In this article, we focused on the bivariate growth curve model with a bilinear spline functional form because it is the most straightforward but useful. The proposed model allows for several extensions. First, the functional form of the trajectories of each endpoint can be generalized to a linear spline with multiple knots or a nonlinear spline (such as a linear-polynomial or a polynomial-polynomial piecewise), which may also show useful in real data analyses. Second, though constructed in the framework of individual measurement occasions, the proposed model considers the same time structure for both repeated outcomes. However, it is accessible to be extended for a joint developmental process with varying time structure of each endpoint thanks to the definition variables approach. It is noted that the same number of repeated measures is not necessary as what is demonstrated for the analysis of the joint development of mathematics and science ability. Third, it is also possible to extend the current work to address a bivariate longitudinal study with dropout under the assumption of missing at random due to the FIML technique. Additionally, we can also extend the PBLSGM to investigate a joint development with at least three constructs. The *OpenMx* and *Mplus 8* syntax that we provided in the online appendix can also be extended accordingly.

References

Bauer, D. J. and Curran, P. J. (2003). Distributional assumptions of growth mixture models: Implications for overextraction of latent trajectory classes. *Psychological Methods*, 8(3):338–363.

Boker, S. M., Neale, M. C., Maes, H. H., Wilde, M. J., Spiegel, M., Brick, T. R., Estabrook, R., Bates, T. C., Mehta, P., von Oertzen, T., Gore, R. J., Hunter, M. D., Hackett, D. C., Karch, J., Brandmaier, A. M., Pritikin, J. N., Zahery, M., Kirkpatrick, R. M., Wang, Y., Driver, C., Massachusetts Institute of Technology, Johnson, S. G., Association for Computing Machinery, Kraft, D., Wilhelm, S., and Manjunath, B. G. (2018). *OpenMx 2.9.6 User Guide*.

Browne, M. W. and du Toit, S. H. C. (1991). Models for learning data. In Collins, L. M. and Horn, J. L., editors, *Best methods for the analysis of change: Recent advances, unanswered questions, future directions*, chapter 4, pages 47–68. American Psychological Association., Washington, DC, US.

Cook, N. R. and Ware, J. H. (1983). Design and analysis methods for longitudinal research. *Annual Review of Public Health*, 4(1):1–23.

Coulombe, P., Selig, J. P., and Delaney, H. D. (2015). Ignoring individual differences in times of assessment in growth curve modeling. *International Journal of Behavioral Development*, 40(1):76–86.

Cudeck, R. and Klebe, K. J. (2002). Multiphase mixed-effects models for repeated measures data. *Psychological Methods*, 7(1):41–63.

Dumenci, L., Perera, R. A., Keefe, F. J., Ang, D. C., J., S., Jensen, M. P., and Riddle, D. L. (2019). Model-based pain and function outcome trajectory types for patients undergoing knee arthroplasty: a secondary analysis from a randomized clinical trial. *Osteoarthritis and cartilage*, 27(6):878–884.

Finkel, D., Reynolds, C., Mcardle, J., Gatz, M., and L Pedersen, N. (2003). Latent growth curve analyses of accelerating decline in cognitive abilities in late adulthood. *Developmental psychology*, 39:535–550.

Flora, D. B. (2008). Specifying piecewise latent trajectory models for longitudinal data. *Structural Equation Modeling: A Multidisciplinary Journal*, 15(3):513–533.

Grimm, K. J., Ram, N., and Estabrook, R. (2016). *Growth Modeling*. Guilford Press.

Harring, J. R., Cudeck, R., and du Toit, S. H. C. (2006). Fitting partially nonlinear random coefficient models as sems. *Multivariate Behavioral Research*, 41(4):579–596.

Hedeker, D. and Gibbons, R. D. (2006). *Longitudinal Data Analysis*. Wiley Series in Probability and Statistics. Wiley.

Hunter, M. D. (2018). State space modeling in an open source, modular, structural equation modeling environment. *Structural Equation Modeling*, 25(2):307–324.

Kohli, N. (2011). *Estimating unknown knots in piecewise linear-linear latent growth mixture models*. PhD thesis, University of Maryland.

Kohli, N. and Harring, J. R. (2013). Modeling growth in latent variables using a piecewise function. *Multivariate Behavioral Research*, 48(3):370–397.

Kohli, N., Harring, J. R., and Hancock, G. R. (2013). Piecewise linear-linear latent growth mixture models with unknown knots. *Educational and Psychological Measurement*, 73(6):935–955.

Kohli, N., Hughes, J., Wang, C., Zopluoglu, C., and Davison, M. L. (2015a). Fitting a linear-linear piecewise growth mixture model with unknown knots: A comparison of two common approaches to inference. *Psychological Methods*, 20(2):259–275.

Kohli, N., Sullivan, A. L., Sadeh, S., and Zopluoglu, C. (2015b). Longitudinal mathematics development of students with learning disabilities and students without disabilities: A comparison of linear, quadratic, and piecewise linear mixed effects models. *Journal of School Psychology*, 53(2):105–120.

Kwok, O., Luo, W., and West, S. G. (2010). Using modification indexes to detect turning points in longitudinal data: A monte carlo study. *Structural Equation Modeling: A Multidisciplinary Journal*, 17(2):216–240.

Lê, T., Norman, G., Tourangeau, K., Brick, J. M., and Mulligan, G. (2011). Early childhood longitudinal study: Kindergarten class of 2010-2011 – sample design issues. *JSM Proceedings*, pages 1629–1639.

Li, F., Duncan, T. E., Duncan, S. C., and Hops, H. (2001). Piecewise growth mixture modeling of adolescent alcohol use data. *Structural Equation Modeling: A Multidisciplinary Journal*, 8(2):175–204.

Liu, J. (2019). *Estimating Knots in Bilinear Spline Growth Models with Time-invariant Covariates in the Framework of Individual Measurement Occasions*. PhD thesis, Virginia Commonwealth University.

Liu, J., Kang, L., Kirkpatrick, R. M., Sabo, R. T., and Perera, R. A. (2019). Estimating knots in bilinear spline growth models with time-invariant covariates in the framework of individual measurement occasions. *arXiv e-prints*, page arXiv:1911.09939.

Marcoulides, K. M. (2018). Automated latent growth curve model fitting: A segmentation and knot selection approach. *Structural Equation Modeling: A Multidisciplinary Journal*, 25(5):687–699.

McArdle, J. (1988). Dynamic but structural equation modeling of repeated measures data. In Nesselroade, J. and Cattell, R., editors, *Handbook of Multivariate Experimental Psychology*, chapter 17, pages 561–614. Springer, Boston, MA.

Mehta, P. D. and Neale, M. C. (2005). People are variables too: Multilevel structural equations modeling. *Psychological Methods*, 10(3):259–284.

Mehta, P. D. and West, S. G. (2000). Putting the individual back into individual growth curves. *Psychological Methods*, 5(1):23–43.

Neale, M. C., Hunter, M. D., Pritikin, J. N., Zahery, M., Brick, T. R., Kirkpatrick, R. M., Estabrook, R., Bates, T. C., Maes, H. H., and Boker, S. M. (2016). OpenMx 2.0: Extended structural equation and statistical modeling. *Psychometrika*, 81(2):535–549.

Preacher, K. J. and Hancock, G. R. (2015). Meaningful aspects of change as novel random coefficients: A general method for reparameterizing longitudinal models. *Psychological Methods*, 20(1):84–101.

Pritikin, J. N., Hunter, M. D., and Boker, S. M. (2015). Modular open-source software for Item Factor Analysis. *Educational and Psychological Measurement*, 75(3):458–474.

Riddle, D. L., Perera, R. A., Jiranek, W. A., and Dumenci, L. (2015). Using surgical appropriateness criteria to examine outcomes of total knee arthroplasty in a united states sample. *Arthritis care & research.*, 67(3):349–357.

Robitaille, A., Muniz, G., Piccinin, A. M., Johansson, B., and Hofer, S. M. (2012). Multivariate longitudinal modeling of cognitive aging: Associations among change and variation in processing speed and visuospatial ability. *GeroPsych*, 25(1):15–24.

Seber, G. A. F. and Wild, C. J. (2003). *Nonlinear Regression*. John Wiley & Sons, Inc.

Sterba, S. K. (2014). Fitting nonlinear latent growth curve models with individually varying time points. *Structural Equation Modeling: A Multidisciplinary Journal*, 21(4):630–647.

Tishler, A. and Zang, I. (1981). A maximum likelihood method for piecewise regression models with a continuous dependent variable. *Journal of the Royal Statistical Society. Series C. Applied Statistics*, 30.

Venables, W. N. and Ripley, B. D. (2002). *Modern Applied Statistics with S*. Springer, New York, fourth edition.

Appendix A Formula Derivation

A.1 The Reparameterizing Procedure for outcome-specific Growth Factors

For each repeated outcome in the original setting of a parallel bilinear spline model, we have three outcome-specific growth factors: an intercept at t_0 ($\eta_0^{[u]}$) and one slope of each stage ($\eta_1^{[u]}$ and $\eta_2^{[u]}$, respectively). To estimate the knot, we may reparameterize these outcome-specific growth factors as the measurement at the knot (i.e., $\eta_{0i}^{[u]} + \eta_{1i}^{[u]} \gamma^{[u]}$), the mean of two slopes (i.e., $\frac{\eta_{1i}^{[u]} + \eta_{2i}^{[u]}}{2}$), and the half difference between two slopes (i.e., $\frac{\eta_{2i}^{[u]} - \eta_{1i}^{[u]}}{2}$) for the i^{th} individual (Seber and Wild, 2003).

=====
 Insert Figure A.1 about here
 =====

Tishler and Zang (1981); Seber and Wild (2003) showed that the continuous two-phase regression model can be written as either the minimum or maximum response value of two trajectories. Liu (2019); Liu et al. (2019) extended such expressions to the BLSGM framework and showed that two possible forms of bilinear spline for the i^{th} individual as such in Figure A.1. In the left panel ($\eta_{1i}^{[y]} > \eta_{2i}^{[y]}$), the measurement y_{ij} should always be the minimum value of two lines and $y_{ij} = \min(\eta_{0i}^{[y]} + \eta_{1i}^{[y]} t_{ij}, \eta_{02i}^{[y]} + \eta_{2i}^{[y]} t_{ij})$. The measurements pre- and post-knot can be unified

$$\begin{aligned}
 y_{ij} &= \min(\eta_{0i}^{[y]} + \eta_{1i}^{[y]} t_{ij}, \eta_{02i}^{[y]} + \eta_{2i}^{[y]} t_{ij}) \\
 &= \frac{1}{2}(\eta_{0i}^{[y]} + \eta_{1i}^{[y]} t_{ij} + \eta_{02i}^{[y]} + \eta_{2i}^{[y]} t_{ij} - |\eta_{0i}^{[y]} + \eta_{1i}^{[y]} t_{ij} - \eta_{02i}^{[y]} - \eta_{2i}^{[y]} t_{ij}|) \\
 &= \frac{1}{2}(\eta_{0i}^{[y]} + \eta_{1i}^{[y]} t_{ij} + \eta_{02i}^{[y]} + \eta_{2i}^{[y]} t_{ij}) - \frac{1}{2}(|\eta_{0i}^{[y]} + \eta_{1i}^{[y]} t_{ij} - \eta_{02i}^{[y]} - \eta_{2i}^{[y]} t_{ij}|) \\
 &= \frac{1}{2}(\eta_{0i}^{[y]} + \eta_{02i}^{[y]} + \eta_{1i}^{[y]} t_{ij} + \eta_{2i}^{[y]} t_{ij}) - \frac{1}{2}(\eta_{1i}^{[y]} - \eta_{2i}^{[y]})|t_{ij} - \gamma^{[y]}| \\
 &= \eta_{0i}^{[y]} + \eta_{1i}^{[y]}(t_{ij} - \gamma^{[y]}) + \eta_{2i}^{[y]}|t_{ij} - \gamma^{[y]}| \\
 &= \eta_{0i}^{[y]} + \eta_{1i}^{[y]}(t_{ij} - \gamma^{[y]}) + \eta_{2i}^{[y]} \sqrt{(t_{ij} - \gamma^{[y]})^2},
 \end{aligned} \tag{A.1}$$

where $\eta_{0i}^{[y]}$, $\eta_{1i}^{[y]}$ and $\eta_{2i}^{[y]}$ are the measurement at the knot, the mean of two slopes, and the half difference between two slopes of the trajectories of the repeated outcome \mathbf{Y} . Through straightforward algebra, the measurement y_{ij} of the bilinear spline in the right panel, where the measurement y_{ij} is always the maximum value of two lines, has the identical final form in Equation A.1. By applying such transformation to each repeated outcome, we obtain the outcome-specific reparameterized growth factors.

A.2 Taylor Series Expansion

Following Liu et al. (2019), for the i^{th} individual, we write a repeated outcome as a function of its trajectory knot, $f(\gamma_i^{[u]})$ and obtain its first derivative with respect to the knot

$$f(\gamma_i^{[u]}) = \eta_{0i}^{[u]} + \eta_{1i}^{[u]}(t_{ij} - \gamma_i^{[u]}) + \eta_{2i}^{[u]} \sqrt{(t_{ij} - \gamma_i^{[u]})^2}$$

and

$$f'(\gamma_i^{[u]}) = \eta_{1i}^{[u]} - \eta_{2i}^{[u]} - \frac{\eta_{2i}^{[u]}(t_{ij} - \gamma_i^{[u]})}{\sqrt{(t_{ij} - \gamma_i^{[u]})^2}} = -\eta_{2i}^{[u]} - \frac{\eta_{2i}^{[u]}(t_{ij} - \gamma_i^{[u]})}{\sqrt{(t_{ij} - \gamma_i^{[u]})^2}},$$

respectively. Then the Taylor series expansion of $f(\gamma_i^{[u]})$ can be expressed as

$$\begin{aligned}
 f(\gamma_i^{[u]}) &= f(\mu_\gamma^{[u]}) + \frac{f'(\mu_\gamma^{[u]})}{1!}(\gamma_i^{[u]} - \mu_\gamma^{[u]}) + \dots \\
 &= \eta_{0i}^{[u]} + \eta_{1i}^{[u]}(t_{ij} - \mu_\gamma^{[u]}) + \eta_{2i}^{[u]} \sqrt{(t_{ij} - \gamma_i^{[u]})^2} + (\gamma_i^{[u]} - \mu_\gamma^{[u]}) \left[-\eta_{2i}^{[u]} - \frac{\eta_{2i}^{[u]}(t_{ij} - \mu_\gamma^{[u]})}{|t_{ij} - \mu_\gamma^{[u]}|} \right] + \dots \\
 &\approx \eta_{0i}^{[u]} + \eta_{1i}^{[u]}(t_{ij} - \mu_\gamma^{[u]}) + \eta_{2i}^{[u]}|t_{ij} - \mu_\gamma^{[u]}| + (\gamma_i^{[u]} - \mu_\gamma^{[u]}) \left[-\mu_{\eta_2'}^{[u]} - \frac{\mu_{\eta_2'}^{[u]}(t_{ij} - \mu_\gamma^{[u]})}{|t_{ij} - \mu_\gamma^{[u]}|} \right],
 \end{aligned}$$

from which we then have the outcome-specific reparameterized growth factors and the corresponding factor loadings for the i^{th} individual.

A.3 Expression of each cell of the re-parameterized mean vector and variance-covariance matrix

$$\begin{aligned}
\mu_{\eta_0}^{[u]} &\approx \mu_{\eta'_0}^{[u]} - \mu_{\gamma}^{[u]} \mu_{\eta'_1}^{[u]} + \mu_{\gamma}^{[u]} \mu_{\eta'_2}^{[u]} \\
\mu_{\eta'_1}^{[u]} &= \mu_{\eta'_1}^{[u]} - \mu_{\eta'_2}^{[u]} \\
\mu_{\eta'_2}^{[u]} &= \mu_{\eta'_2}^{[u]} + \mu_{\eta'_1}^{[u]} \\
\mu_{\gamma}^{[u]} &= \mu_{\gamma}^{[u]} \\
\psi_{00}^{[u]} &\approx (\psi_{11}^{[u]} + \psi_{22}^{[u]} - 2\psi_{12}^{[u]})\mu_{\gamma}^{[u]2} + 2(\psi_{02}^{[u]} - \psi_{01}^{[u]})\mu_{\gamma}^{[u]} + \psi_{00}^{[u]} \\
\psi_{01}^{[u]} &\approx (2\psi_{12}^{[u]} - \psi_{11}^{[u]} - \psi_{22}^{[u]})\mu_{\gamma}^{[u]} + (\psi_{01}^{[u]} - \psi_{02}^{[u]}) \\
\psi_{02}^{[u]} &\approx (\psi_{22}^{[u]} - \psi_{11}^{[u]})\mu_{\gamma}^{[u]} + (\psi_{01}^{[u]} + \psi_{02}^{[u]}) \\
\psi_{0\gamma}^{[u]} &\approx (\psi_{2\gamma}^{[u]} - \psi_{1\gamma}^{[u]})\mu_{\gamma}^{[u]} + \psi_{0\gamma}^{[u]} \\
\psi_{11}^{[u]} &= \psi_{11}^{[u]} + \psi_{22}^{[u]} - 2\psi_{12}^{[u]} \\
\psi_{12}^{[u]} &= \psi_{11}^{[u]} - \psi_{22}^{[u]} \\
\psi_{1\gamma}^{[u]} &= \psi_{1\gamma}^{[u]} - \psi_{2\gamma}^{[u]} \\
\psi_{22}^{[u]} &= \psi_{11}^{[u]} + \psi_{22}^{[u]} + 2\psi_{12}^{[u]} \\
\psi_{2\gamma}^{[u]} &= \psi_{1\gamma}^{[u]} + \psi_{2\gamma}^{[u]} \\
\psi_{\gamma\gamma}^{[u]} &= \psi_{\gamma\gamma}^{[u]} \\
\psi_{00}^{[yz]} &\approx (\psi_{11}^{[yz]} + \psi_{22}^{[yz]} - \psi_{12}^{[yz]} - \psi_{21}^{[yz]})\mu_{\gamma}^{[y]}\mu_{\gamma}^{[z]} + (\psi_{20}^{[yz]} - \psi_{10}^{[yz]})\mu_{\gamma}^{[y]} + (\psi_{02}^{[yz]} - \psi_{01}^{[yz]})\mu_{\gamma}^{[z]} + \psi_{00}^{[yz]} \\
\psi_{01}^{[yz]} &\approx (\psi_{12}^{[yz]} + \psi_{21}^{[yz]} - \psi_{11}^{[yz]} - \psi_{22}^{[yz]})\mu_{\gamma}^{[y]} + (\psi_{01}^{[yz]} - \psi_{02}^{[yz]}) \\
\psi_{02}^{[yz]} &\approx (\psi_{21}^{[yz]} - \psi_{12}^{[yz]} - \psi_{11}^{[yz]} + \psi_{22}^{[yz]})\mu_{\gamma}^{[y]} + (\psi_{01}^{[yz]} + \psi_{02}^{[yz]}) \\
\psi_{0\gamma}^{[yz]} &\approx \psi_{0\gamma}^{[yz]} + (\psi_{2\gamma}^{[yz]} - \psi_{1\gamma}^{[yz]})\mu_{\gamma}^{[y]} \\
\psi_{10}^{[yz]} &\approx (\psi_{12}^{[yz]} + \psi_{21}^{[yz]} - \psi_{11}^{[yz]} - \psi_{22}^{[yz]})\mu_{\gamma}^{[z]} + (\psi_{10}^{[yz]} - \psi_{20}^{[yz]}) \\
\psi_{11}^{[yz]} &= \psi_{11}^{[yz]} - \psi_{21}^{[yz]} - \psi_{12}^{[yz]} + \psi_{22}^{[yz]} \\
\psi_{12}^{[yz]} &= \psi_{11}^{[yz]} - \psi_{21}^{[yz]} + \psi_{12}^{[yz]} - \psi_{22}^{[yz]} \\
\psi_{1\gamma}^{[yz]} &= \psi_{1\gamma}^{[yz]} - \psi_{2\gamma}^{[yz]} \\
\psi_{20}^{[yz]} &\approx (\psi_{12}^{[yz]} - \psi_{21}^{[yz]} - \psi_{11}^{[yz]} + \psi_{22}^{[yz]})\mu_{\gamma}^{[z]} + (\psi_{10}^{[yz]} + \psi_{20}^{[yz]}) \\
\psi_{21}^{[yz]} &= \psi_{11}^{[yz]} - \psi_{22}^{[yz]} - \psi_{12}^{[yz]} - \psi_{21}^{[yz]} \\
\psi_{22}^{[yz]} &= \psi_{11}^{[yz]} + \psi_{22}^{[yz]} + \psi_{12}^{[yz]} + \psi_{21}^{[yz]} \\
\psi_{2\gamma}^{[yz]} &= \psi_{1\gamma}^{[yz]} + \psi_{2\gamma}^{[yz]} \\
\psi_{\gamma 0}^{[yz]} &\approx \psi_{\gamma 0}^{[yz]} + (\psi_{\gamma 2}^{[yz]} - \psi_{\gamma 1}^{[yz]})\mu_{\gamma}^{[z]} \\
\psi_{\gamma 1}^{[yz]} &= \psi_{\gamma 1}^{[yz]} - \psi_{\gamma 2}^{[yz]} \\
\psi_{\gamma 2}^{[yz]} &= \psi_{\gamma 1}^{[yz]} + \psi_{\gamma 2}^{[yz]} \\
\psi_{\gamma\gamma}^{[yz]} &= \psi_{\gamma\gamma}^{[yz]}
\end{aligned}$$

Appendix B More Results

=====

Insert Table B.1 about here

=====

=====

Insert Table B.2 about here

=====

=====

Insert Figure B.1 about here

=====

=====

Insert Figure B.2 about here

=====

=====

Insert Figure B.3 about here

=====

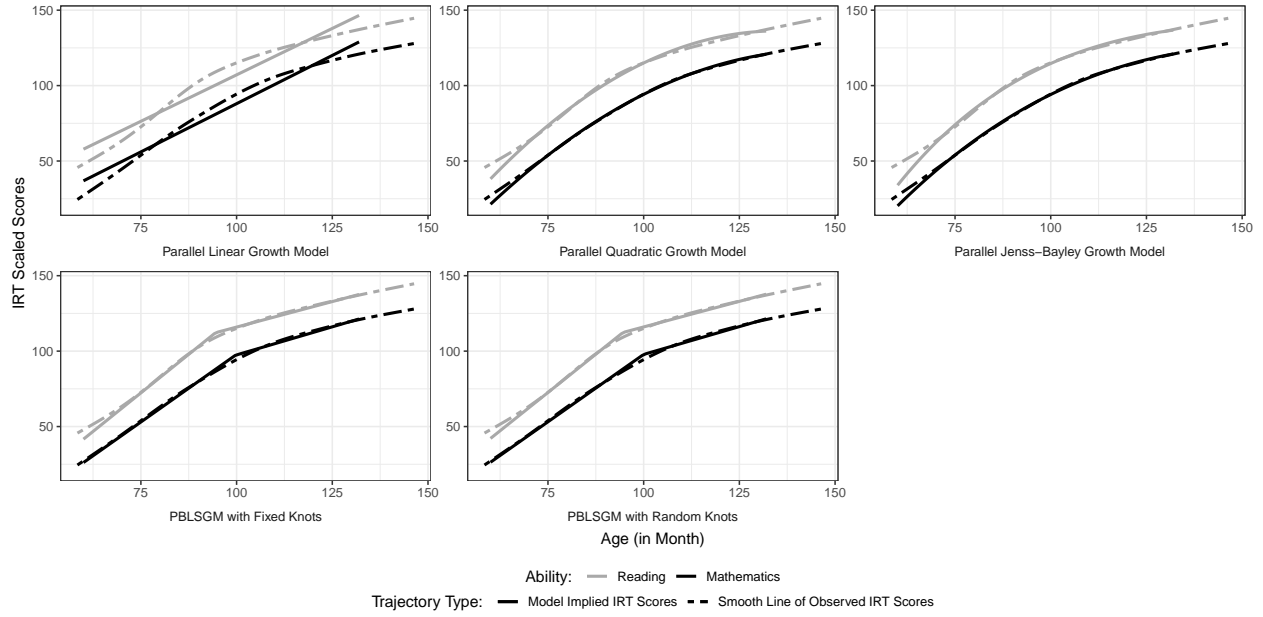


Figure 1: Model Implied Trajectory and Smooth Line of Observed Repeated Outcome

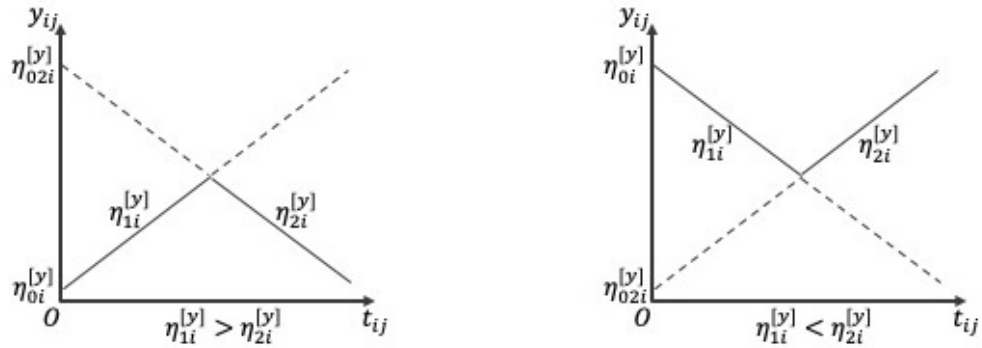


Figure A.1: The Two Forms of the Bilinear Spline (Linear-Linear Piecewise)

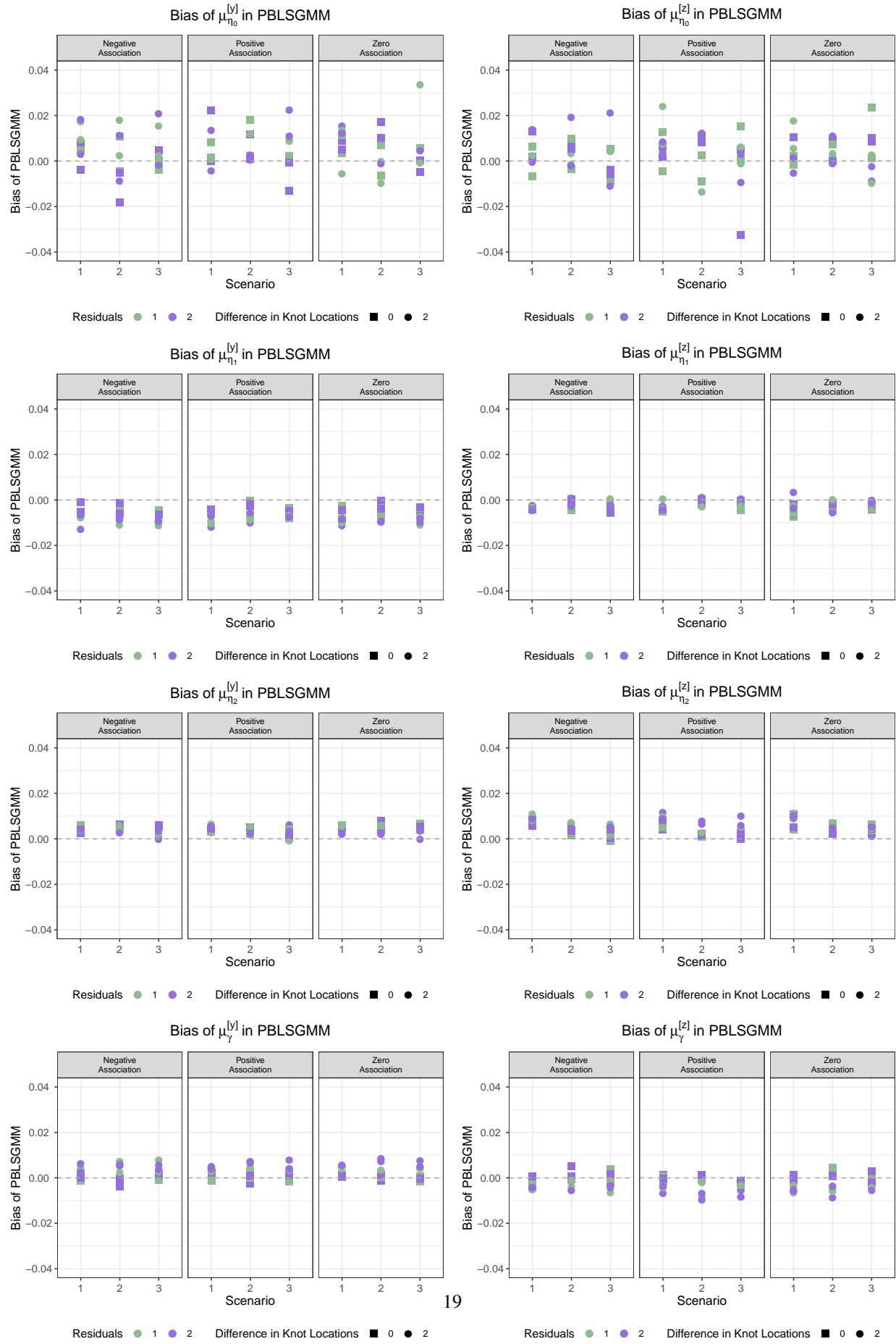


Figure B.1: Biases of Growth Factor Means of PBLSGMM in the ITPs Framework

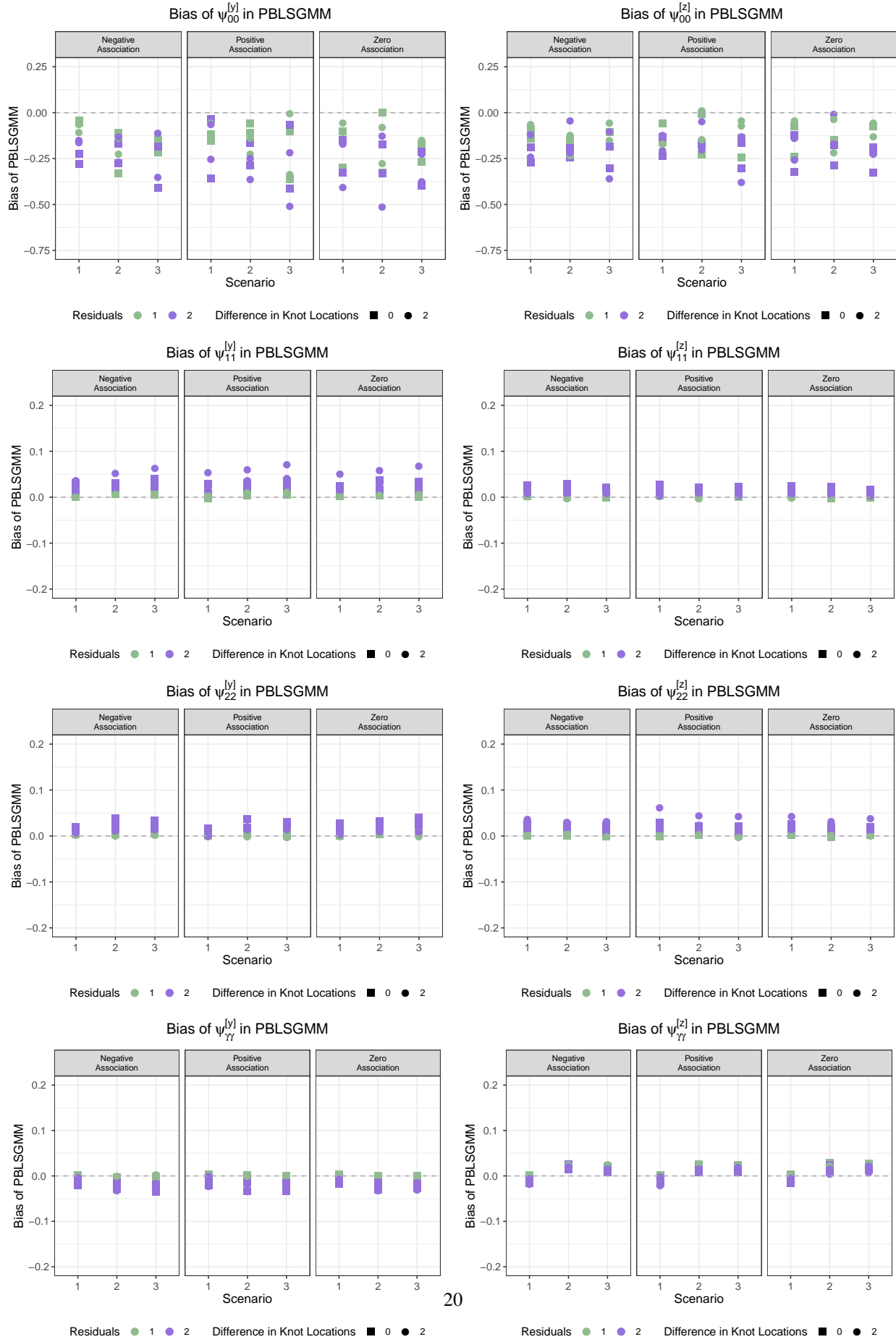


Figure B.2: Biases of Growth Factor Variances of PBLGMM in the ITPs Framework

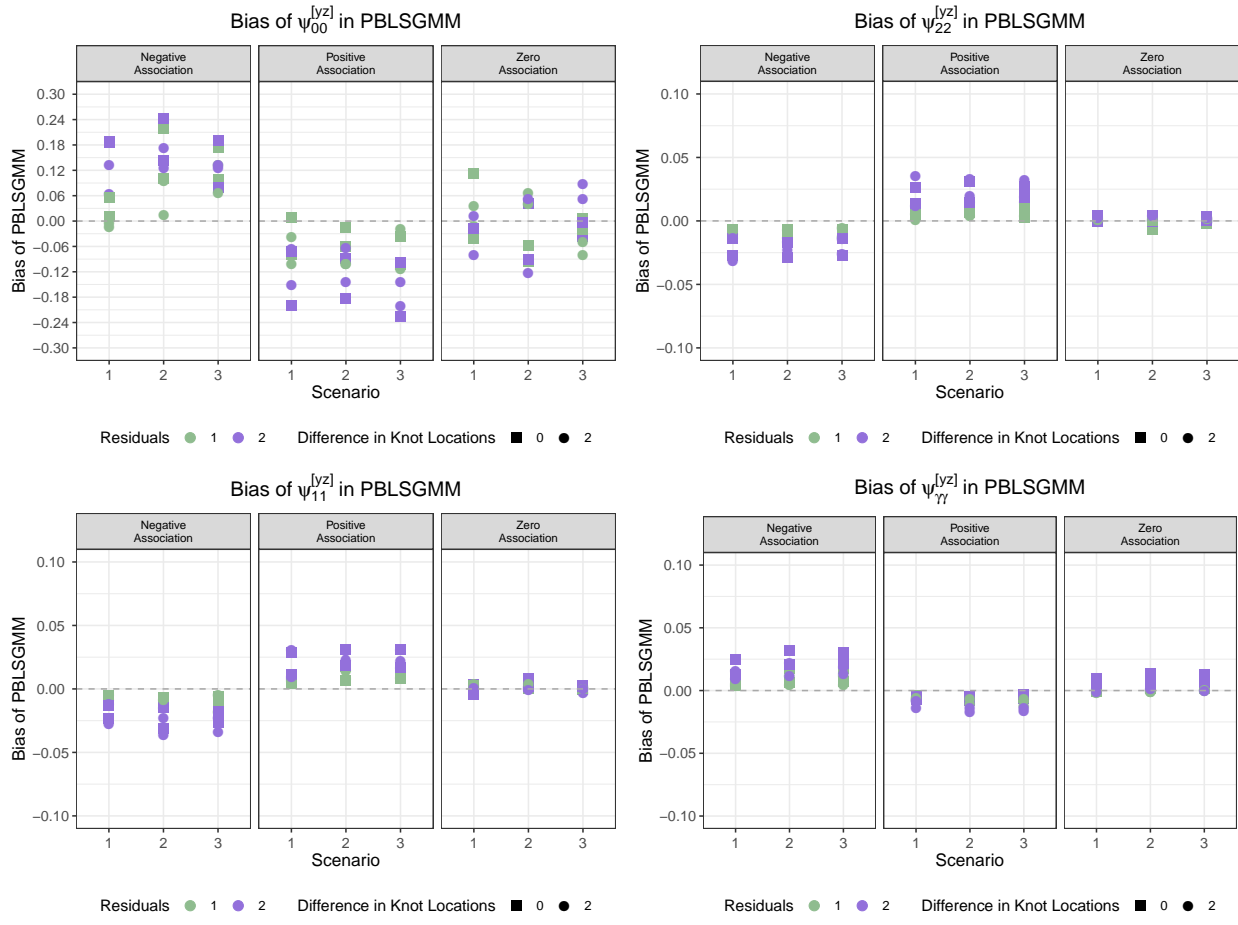


Figure B.3: Biases of Growth Factor Covariances of PBLSGM in the ITPs Framework

Table 1: Simulation Design for PBLSGMs with Unknown Knots in the ITPs Framework

Fixed Conditions	
Variables	Conditions
Intercept Variances	$\psi_{00}^{[u]} = 25 (u = y, z)$
Slope Variances	$\psi_{11}^{[u]} = \psi_{22}^{[u]} = 1 (u = y, z)$
Knot Variances	$\psi_{\gamma\gamma}^{[u]} = 0.09 (u = y, z)$
Correlation of Within-Construct GFs	$\rho^{[u]} = 0.3 (u = y, z)$
Time (t)	10 scaled and equally spaced $t_j (j = 0, \dots, J-1, J = 10)$
Individual t	$t_{ij} \sim U(t_j - \Delta, t_j + \Delta) (j = 0, \dots, J-1; \Delta = 0.25)$
Manipulated Conditions	
Variables	Conditions
Sample Size	$n = 200$ or 500
Knot Locations	$\mu_{\gamma}^{[y]} = 4.50; \mu_{\gamma}^{[z]} = 4.50$ $\mu_{\gamma}^{[y]} = 3.50; \mu_{\gamma}^{[z]} = 5.50$
Correlation of Between-Construct GFs	$\rho = -0.3, 0, 0.3$
Residual Variance	$\theta_{\epsilon}^{[u]} = 1$ or $2 (u = y, z)$
Residual Correlation	$\rho_{\epsilon} = 0.3$
Scenario 1: Different Intercept Mean	
Variables	Conditions
First Slope Means	$\mu_{\eta_1}^{[u]} = 5 (u = y, z)$
Second Slope Means	$\mu_{\eta_2}^{[u]} = 2.6 (u = y, z)$
Intercept Means	$\mu_{\eta_0}^{[y]} = 98, \mu_{\eta_0}^{[z]} = 102$
Scenario 2: Different First Slope Mean	
Variables	Conditions
Intercept Means	$\mu_{\eta_0}^{[u]} = 100 (u = y, z)$
Second Slope Means	$\mu_{\eta_2}^{[u]} = 2 (u = y, z)$
First Slope Means	$\mu_{\eta_1}^{[y]} = 4.4, \mu_{\eta_1}^{[z]} = 3.6$
Scenario 3: Different Second Slope Mean	
Variables	Conditions
Intercept Means	$\mu_{\eta_0}^{[u]} = 100 (u = y, z)$
First Slope Means	$\mu_{\eta_1}^{[u]} = 5 (u = y, z)$
Second Slope Means	$\mu_{\eta_2}^{[y]} = 2.6, \mu_{\eta_2}^{[z]} = 3.4$

Table 2: Number of Improper Solutions among 1,000 Replications of the PBLSGMs in the ITPs Framework

			$\theta_{\epsilon}^{[u]} = 1$		$\theta_{\epsilon}^{[u]} = 2$	
			$n = 200$	$n = 500$	$n = 200$	$n = 500$
Positive Between-Construct Correlation $\rho = 0.3$	Same Knot Locations	Scenario 1	11//55 ¹	0//1	188//217	39//92
		Scenario 2	88//111	5//17	292//277	134//118
		Scenario 3	105//112	10//17	291//266	122//132
	Different Knot Locations	Scenario 1	17//59	1//3	180//261	25//77
		Scenario 2	70//132	11//21	311//243	133//139
		Scenario 3	74//120	10//15	288//269	119//147
Negative Between-Construct Correlation $\rho = -0.3$	Same Knot Locations	Scenario 1	17//100	1//12	172//239	36//124
		Scenario 2	88//130	10//46	267//269	105//163
		Scenario 3	73//143	8//45	327//251	135//159
	Different Knot Locations	Scenario 1	14//62	0//3	167//232	25//100
		Scenario 2	77//132	4//26	290//258	114//143
		Scenario 3	86//139	7//15	295//242	111//154
Zero Between-Construct Correlation $\rho = 0$	Same Knot Locations	Scenario 1	16//59	0//0	187//209	40//83
		Scenario 2	76//109	11//15	315//250	100//125
		Scenario 3	67//114	7//23	294//222	151//129
	Different Knot Locations	Scenario 1	13//41	0//1	161//203	36//84
		Scenario 2	74//75	14//17	311//246	122//145
		Scenario 3	85//87	9//15	303//223	121//114

¹ 11//55 indicates that among 1,000 convergent replications of the PBLSGM, we have 11 and 55 improper solutions due to negative knot variances and out-of-range correlations of the knot with other growth factors, respectively.

Table 3: Median (Range) of the Bias of Each Parameter in PBLSGM in the ITPs Framework

	Para.	Reduced PBLSGM		Full PBLSGM	
		Median	(Range)	Median	(Range)
Grow Factor Means of Y	$\mu_{\eta_0}^{[y]}$	0.0048	(-0.0181, 0.0359)	0.0040	(-0.0183, 0.0334)
	$\mu_{\eta_1}^{[y]}$	-0.0081	(-0.0147, -0.0002)	-0.0068	(-0.0130, -0.0002)
	$\mu_{\eta_2}^{[y]}$	0.0034	(-0.0030, 0.0081)	0.0038	(-0.0010, 0.0080)
	$\mu_{\gamma}^{[y]}$	0.0047	(-0.0034, 0.0131)	0.0023	(-0.0037, 0.0085)
Grow Factor Variances of Y	$\psi_{00}^{[y]}$	-0.4826	(-0.7218, -0.3349)	-0.1725	(-0.5142, 0.0007)
	$\psi_{11}^{[y]}$	0.0856	(0.0626, 0.1278)	0.0168	(-0.0025, 0.0712)
	$\psi_{22}^{[y]}$	0.0557	(0.0351, 0.0768)	0.0092	(-0.0027, 0.0401)
	$\psi_{\gamma\gamma}^{[y]}$	-0.0900	(-0.0900, -0.0900)	-0.0128	(-0.0345, 0.0028)
Grow Factor Means of Z	$\mu_{\eta_0}^{[z]}$	0.0024	(-0.0318, 0.0238)	0.0037	(-0.0324, 0.0239)
	$\mu_{\eta_1}^{[z]}$	-0.0020	(-0.0072, 0.0043)	-0.0026	(-0.0074, 0.0034)
	$\mu_{\eta_2}^{[z]}$	0.0059	(-0.0006, 0.0147)	0.0050	(-0.0009, 0.0117)
	$\mu_{\gamma}^{[z]}$	-0.0044	(-0.0134, 0.0059)	-0.0020	(-0.0097, 0.0050)
Grow Factor Variances of Z	$\psi_{00}^{[z]}$	-0.3763	(-0.5742, -0.1107)	-0.1604	(-0.3786, 0.0089)
	$\psi_{11}^{[z]}$	0.0415	(0.0146, 0.0767)	0.0068	(-0.0034, 0.0289)
	$\psi_{22}^{[z]}$	0.0677	(0.0395, 0.1314)	0.0118	(-0.0026, 0.0614)
	$\psi_{\gamma\gamma}^{[z]}$	-0.0900	(-0.0900, -0.0900)	0.0152	(-0.0222, 0.0284)
Grow Factor Covariances of Y and Z	$\psi_{00}^{[yz]}$	-0.0190	(-0.4455, 0.4793)	-0.0128	(-0.2265, 0.2425)
	$\psi_{11}^{[yz]}$	0.0014	(-0.0707, 0.0739)	0.0016	(-0.0363, 0.0313)
	$\psi_{22}^{[yz]}$	0.0016	(-0.0733, 0.0768)	0.0005	(-0.0316, 0.0357)
	$\psi_{\gamma\gamma}^{[yz]}$	-0.0270	(-0.0270, -0.0270)	0.0008	(-0.0172, 0.0319)

Table 4: Median (Range) of the RMSE of Each Parameter in PBLSGM in the ITPs Framework

	Para.	Reduced PBLSGM	Full PBLSGM
		Median (Range)	Median (Range)
Grow Factor Means of Y	$\mu_{\eta_0}^{[y]}$	0.2908(0.2213, 0.3707)	0.2908(0.2216, 0.3707)
	$\mu_{\eta_1}^{[y]}$	0.0641(0.0448, 0.0855)	0.0643(0.0448, 0.0857)
	$\mu_{\eta_2}^{[y]}$	0.0609(0.0448, 0.0810)	0.0612(0.0450, 0.0815)
	$\mu_{\gamma}^{[y]}$	0.0387(0.0266, 0.0590)	0.0392(0.0269, 0.0597)
Grow Factor Variances of Y	$\psi_{00}^{[y]}$	2.1331(1.5840, 2.7300)	2.1094(1.5649, 2.7266)
	$\psi_{11}^{[y]}$	0.1361(0.0988, 0.1821)	0.1086(0.0682, 0.1628)
	$\psi_{22}^{[y]}$	0.1104(0.0784, 0.1430)	0.0954(0.0659, 0.1320)
	$\psi_{\gamma\gamma}^{[y]}$	0.0900(0.0900, 0.0900)	0.0522(0.0245, 0.0790)
Grow Factor Means of Z	$\mu_{\eta_0}^{[z]}$	0.2906(0.2189, 0.3788)	0.2906(0.2191, 0.3788)
	$\mu_{\eta_1}^{[z]}$	0.0600(0.0444, 0.0794)	0.0605(0.0447, 0.0795)
	$\mu_{\eta_2}^{[z]}$	0.0634(0.0453, 0.0845)	0.0634(0.0456, 0.0848)
	$\mu_{\gamma}^{[z]}$	0.0467(0.0263, 0.0746)	0.0511(0.0263, 0.0812)
Grow Factor Variances of Z	$\psi_{00}^{[z]}$	2.0967(1.5998, 2.6670)	2.0766(1.5775, 2.6800)
	$\psi_{11}^{[z]}$	0.1048(0.0687, 0.1388)	0.0916(0.0637, 0.1294)
	$\psi_{22}^{[z]}$	0.1210(0.0806, 0.1872)	0.1026(0.0674, 0.1587)
	$\psi_{\gamma\gamma}^{[z]}$	0.0900(0.0900, 0.0900)	0.0799(0.0249, 0.1313)
Grow Factor Covariances of Y and Z	$\psi_{00}^{[yz]}$	1.5379(1.0940, 1.9753)	1.5379(1.1071, 1.9817)
	$\psi_{11}^{[yz]}$	0.0865(0.0489, 0.1146)	0.0731(0.0481, 0.1031)
	$\psi_{22}^{[yz]}$	0.0840(0.0501, 0.1227)	0.0710(0.0484, 0.1074)
	$\psi_{\gamma\gamma}^{[yz]}$	0.0900(0.0900, 0.0900)	0.0348(0.0166, 0.0561)

Table 5: Median (Range) of the Coverage Probability of Each Parameter in PBLGSM in the ITPs Framework

	Para.	Reduced PBLGSM	Full PBLGSM
		Median (Range)	Median (Range)
Grow Factor Means of Y	$\mu_{\eta_0}^{[y]}$	0.9455(0.9200, 0.9590)	0.9484(0.9153, 0.9656) ¹
	$\mu_{\eta_1}^{[y]}$	0.9550(0.9410, 0.9710)	0.9468(0.9196, 0.9626)
	$\mu_{\eta_2}^{[y]}$	0.9535(0.9380, 0.9670)	0.9478(0.9276, 0.9635)
	$\mu_{\gamma}^{[y]}$	0.9040(0.8560, 0.9340)	0.9500(0.9216, 0.9675)
Grow Factor Variances of Y	$\psi_{00}^{[y]}$	0.9280(0.9110, 0.9500)	0.9452(0.9254, 0.9597)
	$\psi_{11}^{[y]}$	0.8865(0.6610, 0.9490)	0.9496(0.9311, 0.9655)
	$\psi_{22}^{[y]}$	0.9355(0.8450, 0.9630)	0.9476(0.9303, 0.9619)
	$\psi_{\gamma\gamma}^{[y]}$	0.0000(0.0000, 0.0000)	0.9772(0.9440, 0.9954)
Grow Factor Means of Z	$\mu_{\eta_0}^{[z]}$	0.9470(0.9290, 0.9620)	0.9486(0.9265, 0.9664)
	$\mu_{\eta_1}^{[z]}$	0.9520(0.9360, 0.9630)	0.9466(0.9244, 0.9662)
	$\mu_{\eta_2}^{[z]}$	0.9540(0.9370, 0.9670)	0.9492(0.9249, 0.9662)
	$\mu_{\gamma}^{[z]}$	0.9110(0.8460, 0.9450)	0.9528(0.9367, 0.9763)
Grow Factor Variances of Z	$\psi_{00}^{[z]}$	0.9340(0.9180, 0.9480)	0.9437(0.9249, 0.9586)
	$\psi_{11}^{[z]}$	0.9460(0.8570, 0.9670)	0.9458(0.9148, 0.9664)
	$\psi_{22}^{[z]}$	0.9285(0.6640, 0.9610)	0.9492(0.9276, 0.9662)
	$\psi_{\gamma\gamma}^{[z]}$	0.0000(0.0000, 0.0000)	0.9712(0.9343, 0.9889)
Grow Factor Covariances of Y and Z	$\psi_{00}^{[yz]}$	0.9405(0.9190, 0.9610)	0.9483(0.9306, 0.9696)
	$\psi_{11}^{[yz]}$	0.9140(0.7360, 0.9610)	0.9492(0.9206, 0.9684)
	$\psi_{22}^{[yz]}$	0.9175(0.7330, 0.9630)	0.9516(0.9333, 0.9673)
	$\psi_{\gamma\gamma}^{[yz]}$	0.0000(0.0000, 0.0000)	0.9678(0.9329, 0.9919)

¹ For the full PBLGSM, the reported coverage probabilities have four decimals since we calculated the coverage probabilities only based on the replications with proper solutions.

Table 6: Summary of Model Fit Information For the Joint Development Model of Reading and Mathematics Ability

Model	-2loglikelihood	AIC	BIC	# of Para.	Reading Res.	Math Res.	Res. Covariance
Parallel Linear	53915.82	53950	54018	17	120.36	74.58	59.01
Parallel Quadratic	50658.72	50719	50838	30	48.05	31.96	6.04
Parallel Jenss-Bayley	50588.74	50653	50780	32	46.10	32.04	5.89
Reduced PBLGSM	50586.42	50650	50778	32	44.57	33.43	7.42
Full PBLGSM	50437.79	50532	50719	47	42.93	31.94	6.87

Table 7: Estimates of Parallel Bilinear Spline Growth Model for Reading and Mathematics Ability

	Reading IRT Scores		Math IRT Scores		Covariances	
Mean	Estimate (SE)	P value	Estimate (SE)	P value	Estimate (SE)	P value
Intercept ¹	42.137(0.753)	< 0.0001 ²	26.355(0.584)	< 0.0001*	— ³	—
Slope 1	2.030(0.028)	< 0.0001*	1.787(0.019)	< 0.0001*	—	—
Slope 2	0.678(0.015)	< 0.0001*	0.737(0.017)	< 0.0001*	—	—
Knot	94.606(0.361)	< 0.0001*	99.989(0.439)	< 0.0001*	—	—
Variance	Estimate (SE)	P value	Estimate (SE)	P value	Estimate (SE)	P value
Intercept	172.249(16.626)	< 0.0001*	104.242(10.001)	< 0.0001*	100.337(10.648)	< 0.0001*
Slope 1	0.207(0.023)	< 0.0001*	0.086(0.010)	< 0.0001*	0.085(0.012)	< 0.0001*
Slope 2	0.021(0.006)	0.0005*	0.033(0.008)	< 0.0001*	0.009(0.005)	0.0719
Knot	10.597(3.801)	0.0053*	16.984(5.705)	0.0029*	7.863(3.202)	0.0141*

¹ Intercept was defined as 60-month old in this case.

² * indicates statistical significance at 0.05 level.

³ — indicates that the metric was not available for the model.

Table 8: Summary of Model Fit Information For the Joint Development Model of Mathematics and Science Ability

Model	-2loglikelihood	AIC	BIC	# of Para.	Math Res.	Science Res.	Res. Covariance
Reduced PBLSGM	45184.78	45249	45377	32	33.25	19.26	2.44
Full PBLSGM	45123.20	45217	45404	47	31.69	18.80	2.14
Mixed PBLSGM	45132.07	45210	45366	39	31.75	19.28	2.45

Table 9: Estimates of Parallel Bilinear Spline Growth Model for Mathematics and Science Ability

	Math IRT Scores		Science IRT Scores		Covariances	
Mean	Estimate (SE)	P value	Estimate (SE)	P value	Estimate (SE)	P value
Intercept ¹	26.467(0.589)	< 0.0001 ²	22.055(0.426)	< 0.0001*	— ³	—
Slope 1	1.777(0.019)	< 0.0001*	0.839(0.015)	< 0.0001*	—	—
Slope 2	0.729(0.017)	< 0.0001*	0.575(0.013)	< 0.0001*	—	—
Knot	100.365(0.445)	< 0.0001*	100.081(0.948)	< 0.0001*	—	—
Variance	Estimate (SE)	P value	Estimate (SE)	P value	Estimate (SE)	P value
Intercept	106.483(10.168)	< 0.0001*	36.673(4.897)	< 0.0001*	40.554(5.468)	< 0.0001*
Slope 1	0.086(0.010)	< 0.0001*	0.046(0.006)	< 0.0001*	0.038(0.006)	< 0.0001*
Slope 2	0.032(0.008)	0.0001*	0.022(0.004)	< 0.0001*	0.007(0.004)	0.0801
Knot	17.650(6.007)	0.0033*	—	—	—	—

¹ Intercept of mathematics and science ability were both defined as 60-month old in this case. Therefore, the intercept of science ability is pseudo-intercept since the estimated science IRT scaled scores prior to the second round (minimum age at the second round is around 64-month old) were extrapolated.

² * indicates statistical significance at 0.05 level.

³ — indicates that the metric was not available for the model.

Table B.1: Median (Range) of the Relative Bias of Each Parameter in PBLSGM in the ITPs Framework

	Para.	Reduced PBLSGM	Full PBLSGM
		Median (Range)	Median (Range)
Grow Factor Means of Y	$\mu_{\eta_0}^{[y]}$	0.0000(−0.0002, 0.0004)	0.0000(−0.0002, 0.0003)
	$\mu_{\eta_1}^{[y]}$	0.0016(−0.0031, 0.0000)	−0.0014(−0.0026, 0.0000)
	$\mu_{\eta_2}^{[y]}$	0.0014(−0.0011, 0.0040)	0.0016(−0.0004, 0.0040)
	$\mu_{\gamma}^{[y]}$	0.0012(−0.0008, 0.0037)	0.0005(−0.0008, 0.0024)
Grow Factor Variances of Y	$\psi_{00}^{[y]}$	−0.0193(−0.0289, −0.0134)	−0.0069(−0.0206, 0.0000)
	$\psi_{11}^{[y]}$	0.0856(0.0626, 0.1278)	0.0168(−0.0025, 0.0712)
	$\psi_{22}^{[y]}$	0.0557(0.0351, 0.0768)	0.0092(−0.0027, 0.0401)
	$\psi_{\gamma\gamma}^{[y]}$	−1.0000(−1.0000, −1.0000)	−0.1416(−0.3829, 0.0309)
Grow Factor Means of Z	$\mu_{\eta_0}^{[z]}$	0.0000(−0.0003, 0.0002)	0.0000(−0.0003, 0.0002)
	$\mu_{\eta_1}^{[z]}$	−0.0005(−0.0014, 0.0009)	−0.0006(−0.0015, 0.0007)
	$\mu_{\eta_2}^{[z]}$	0.0020(−0.0002, 0.0057)	0.0019(−0.0003, 0.0045)
	$\mu_{\gamma}^{[z]}$	−0.0008(−0.0024, 0.0013)	−0.0004(−0.0018, 0.0011)
Grow Factor Variances of Z	$\psi_{00}^{[z]}$	−0.0150(−0.0230, −0.0044)	−0.0064(−0.0151, 0.0004)
	$\psi_{11}^{[z]}$	0.0415(0.0146, 0.0767)	0.0068(−0.0034, 0.0289)
	$\psi_{22}^{[z]}$	0.0677(0.0395, 0.1314)	0.0118(−0.0026, 0.0614)
	$\psi_{\gamma\gamma}^{[z]}$	−1.0000(−1.0000, −1.0000)	0.1689(−0.2463, 0.3152)
Grow Factor Covariances of Y and Z	$\psi_{00}^{[yz]}$	−0.0468(−∞, ∞)	−0.0136(−∞, ∞)
	$\psi_{11}^{[yz]}$	0.2200(−∞, ∞)	0.0599(−∞, ∞)
	$\psi_{22}^{[yz]}$	0.1966(−∞, ∞)	0.0465(−∞, ∞)
	$\psi_{\gamma\gamma}^{[yz]}$	−1.0000(−∞, ∞)	−0.2634(−∞, ∞)

Table B.2: Median (Range) of the Relative RMSE of Each Parameter in PBLSGM in the ITPs Framework

	Para.	Reduced PBLSGM Median (Range)	Full PBLSGM Median (Range)
Grow Factor Means of Y	$\mu_{\eta_0}^{[y]}$	0.0029(0.0022, 0.0038)	0.0029(0.0022, 0.0038)
	$\mu_{\eta_1}^{[y]}$	0.0136(0.0091, 0.0194)	0.0136(0.0091, 0.0195)
	$\mu_{\eta_2}^{[y]}$	0.0262(0.0175, 0.0405)	0.0262(0.0176, 0.0407)
	$\mu_{\gamma}^{[y]}$	0.0098(0.0059, 0.0169)	0.0100(0.0061, 0.0171)
Grow Factor Variances of Y	$\psi_{00}^{[y]}$	0.0853(0.0634, 0.1092)	0.0844(0.0626, 0.1091)
	$\psi_{11}^{[y]}$	0.1361(0.0988, 0.1821)	0.1086(0.0682, 0.1628)
	$\psi_{22}^{[y]}$	0.1104(0.0784, 0.1430)	0.0954(0.0659, 0.1320)
	$\psi_{\gamma\gamma}^{[y]}$	1.0000(1.0000, 1.0000)	0.5802(0.2728, 0.8778)
Grow Factor Means of Z	$\mu_{\eta_0}^{[z]}$	0.0028(0.0022, 0.0037)	0.0028(0.0022, 0.0037)
	$\mu_{\eta_1}^{[z]}$	0.0140(0.0089, 0.0221)	0.0140(0.0089, 0.0221)
	$\mu_{\eta_2}^{[z]}$	0.0236(0.0133, 0.0423)	0.0238(0.0134, 0.0424)
	$\mu_{\gamma}^{[z]}$	0.0099(0.0051, 0.0166)	0.0101(0.0049, 0.018)
Grow Factor Variances of Z	$\psi_{00}^{[z]}$	0.0839(0.0640, 0.1067)	0.0831(0.0631, 0.1072)
	$\psi_{11}^{[z]}$	0.1048(0.0687, 0.1388)	0.0916(0.0637, 0.1294)
	$\psi_{22}^{[z]}$	0.1210(0.0806, 0.1872)	0.1026(0.0674, 0.1587)
	$\psi_{\gamma\gamma}^{[z]}$	1.0000(1.0000, 1.0000)	0.8881(0.2763, 1.4587)
Grow Factor Covariances of Y and Z	$\psi_{00}^{[yz]}$	0.2100(−0.2634, ∞)	0.2088(−0.2642, ∞)
	$\psi_{11}^{[yz]}$	0.3192(−0.3820, ∞)	0.2496(−0.3438, ∞)
	$\psi_{22}^{[yz]}$	0.3162(−0.3846, ∞)	0.2465(−0.3378, ∞)
	$\psi_{\gamma\gamma}^{[yz]}$	−1.0000(−1.0000, ∞)	1.3182(−2.0787, ∞)